THE JOURNAL OF BIOLOGICAL CHEMISTRY VOL. 288, NO. 28, pp. 20135–20150, July 12, 2013
Published in the U.S.A.

Enhanced Fasting Glucose Turnover in Mice with Disrupted Action of TUG Protein in Skeletal Muscle*

Received for publication, January 30, 2013, and in revised form, June 4, 2013 Published, JBC Papers in Press, June 6, 2013, DOI 10.1074/jbc.M113.458075

Michael G. Löffler[‡], Andreas L. Birkenfeld[‡1], Katerina M. Philbrick[‡], Jonathan P. Belman[‡§], Estifanos N. Habtemichael[‡], Carmen J. Booth[¶], Carlos M. Castorena[‖], Cheol Soo Choi[‡], Francois R. Jornayvaz[‡], Brandon M. Gassaway[**], Hui-Young Lee[‡], Gregory D. Cartee[‖], William Philbrick[‡], Gerald I. Shulman[‡‡‡], Varman T. Samuel[‡§§], and Jonathan S. Bogan[‡§2]**

*From the [‡]Section of Endocrinology and Metabolism, Department of Internal Medicine, Departments of [§]Cell Biology and [**]Cellular and Molecular Physiology, [¶]*Section of Comparative Medicine, and [‡‡]*Howard Hughes Medical Institute, Yale University School of Medicine, New Haven, Connecticut 06520-8020, [‖]Muscle Biology Laboratory, School of Kinesiology, University of Michigan, Ann Arbor, Michigan 48109, and [§§]Veterans Affairs Medical Center, West Haven, Connecticut 06516*

Background: Insulin stimulates endoproteolytic cleavage of TUG proteins to promote glucose uptake in cultured adipocytes, but the role of this pathway in muscle is uncharacterized.
Results: Transgenic mice with constitutive and unregulated TUG cleavage in muscle had increased whole-body and muscle-specific glucose uptake during fasting.
Conclusion: Insulin acts through TUG to control glucose uptake in muscle.
Significance: Understanding insulin action will elucidate diabetes pathogenesis.

Insulin stimulates glucose uptake in 3T3-L1 adipocytes in part by causing endoproteolytic cleavage of TUG (tether containing a ubiquitin regulatory X (UBX) domain for glucose transporter 4 (GLUT4)). Cleavage liberates intracellularly sequestered GLUT4 glucose transporters for translocation to the cell surface. To test the role of this regulation in muscle, we used mice with muscle-specific transgenic expression of a truncated TUG fragment, UBX-Cter. This fragment causes GLUT4 translocation in unstimulated 3T3-L1 adipocytes. We predicted that transgenic mice would have GLUT4 translocation in muscle during fasting. UBX-Cter expression caused depletion of PIST (PDZ domain protein interacting specifically with TC10), which transmits an insulin signal to TUG. Whereas insulin stimulated TUG proteolysis in control muscles, proteolysis was constitutive in transgenic muscles. Fasting transgenic mice had decreased plasma glucose and insulin concentrations compared with controls. Whole-body glucose turnover was increased during fasting but not during hyperinsulinemic clamp studies. In muscles with the greatest UBX-Cter expression, 2-deoxyglucose uptake during fasting was similar to that in control muscles during hyperinsulinemic clamp studies. Fasting transgenic mice had increased muscle glycogen, and GLUT4 targeting to T-tubule fractions was increased 5.7-fold. Whole-body oxygen consumption (VO_2), carbon dioxide production (VCO_2), and energy expenditure were increased by 12–13%. After 3 weeks on a high fat diet, the decreased fasting plasma glucose in transgenic mice compared with controls was more marked, and increased glucose turnover was not observed; the transgenic mice continued to have an increased metabolic rate. We conclude that insulin stimulates TUG proteolysis to translocate GLUT4 in muscle, that this pathway impacts systemic glucose homeostasis and energy metabolism, and that the effects of activating this pathway are maintained during high fat diet-induced insulin resistance in mice.

Glucose transport into cells is the main, rate-controlling step for overall glucose utilization in skeletal muscle. Transport is mediated primarily by GLUT4[3] transporters and is dysregulated in type 2 diabetes (1, 2). GLUT4 is retained intracellularly in cells not stimulated with insulin and undergoes exocytic translocation to the cell surface in response to insulin stimulation (3). By increasing the number of transporters present in the plasma membrane, GLUT4 translocation augments glucose uptake. The ability of insulin to promote GLUT4 translocation is reduced in insulin resistance (4). This reflects the action of ectopic lipid metabolites to impede insulin signaling and possibly alter GLUT4 targeting within unstimulated cells (3, 5–7). Impaired GLUT4 translocation is critical to the pathogenesis of metabolic syndrome (4, 8). However, the trafficking pathways and biochemical mechanisms that regulate GLUT4 targeting remain poorly understood.

Our previous data support a model in which insulin acts to relieve a negative regulator of glucose uptake. In unstimulated

* This work was supported, in whole or in part, by National Institutes of Health Grants DK075772 and DK092661 (to J. S. B); DK071771 (to G. D. C.); DK40936 (to G. I. S.); T32GM007205, TL1RR024137, and F30DK093198 (to J. P. B); and T32DK007058 (to E. N. H.). This work was also supported by American Diabetes Association Grant 1-12-BS-16 and the W. M. Keck Foundation (to J. S. B.).
[1] Supported by German Research Foundation Grant BI1292/4-1.
[2] To whom correspondence should be addressed: Section of Endocrinology and Metabolism, Dept. of Internal Medicine, Yale University School of Medicine, P. O. Box 208020, New Haven, CT 06520-8020. Tel.: 203-785-6319; Fax: 203-785-6462; E-mail: jonathan.bogan@yale.edu.

[3] The abbreviations used are: GLUT, glucose transporter; 2DOG, 2-deoxy-D-glucose; GSV, GLUT4 storage vesicle; HFD, high fat diet; TUG, tether containing a UBX domain for GLUT4; UBX, ubiquitin regulatory X; VO_2, oxygen consumption; VCO_2, carbon dioxide production; Q-PCR, quantitative real time PCR; RER, respiratory exchange ratio; TG, transgenic; PIST, PDZ domain protein interacting specifically with TC10; hGH, human growth hormone.

cells, GLUT4 accumulates in intracellular vesicles termed "GLUT4 storage vesicles" (GSVs), which sequester the transporters away from the cell surface (9, 10). Best described in adipocytes, GSVs lack endosome and Golgi marker proteins and are mobilized acutely by insulin stimulation. We identified TUG as a GLUT4-regulating protein and proposed that it traps GSVs intracellularly in unstimulated adipocytes (11). Insulin releases these vesicles from TUG to promote GLUT4 translocation. Data from 3T3-L1 adipocytes show that this mechanism is a major site of insulin action to regulate GLUT4 trafficking and glucose uptake (12, 13). TUG resides at the *cis* side of the Golgi complex and links GLUT4-containing vesicles to Golgi matrix proteins present at this location (14, 15). Insulin signals through the TC10α GTPase and its effector, PIST, to stimulate TUG endoproteolytic cleavage, which liberates the vesicles and is required for highly insulin-responsive GLUT4 translocation and glucose uptake (15). This pathway is coordinated with insulin signals through Akt2 to AS160/Tbc1D4 and (in muscle) Tbc1D1, which modulate specific Rab GTPases, as well as with signals to promote vesicle fusion at the plasma membrane (16–22). During continuous insulin exposure, GLUT4 is carried to the surface in vesicles distinct from those mobilized by acute insulin stimulation, and the GSV compartment is bypassed (13). This arrangement permits the discharge of discrete amounts of GLUT4 from a sequestered intracellular pool to a cell surface recycling pathway as insulin concentrations vary over a physiologic range (3, 23–25).

The model described above is based primarily on work in cultured cells, and until now its relevance in skeletal muscle *in vivo* has not been tested. Insulin stimulates the dissociation of TUG-GLUT4 complexes in muscle as in fat (26). Moreover, TUG and GLUT4 abundances correlate across diverse muscle types possibly because TUG controls the stability as well as targeting of GLUT4 proteins (12, 27). Here, we studied the role of TUG to control GLUT4 localization and glucose uptake in muscle. We used a skeletal muscle-specific promoter to express a dominant negative fragment of TUG, UBX-Cter, in transgenic mice. This truncated protein inhibits the ability of endogenous intact TUG protein to sequester GLUT4 at the Golgi matrix. In 3T3-L1 adipocytes, the UBX-Cter protein causes GLUT4 translocation and glucose uptake in the absence of insulin stimulation, mimicking the effects of insulin or of TUG RNAi (12). Data herein show that UBX-Cter similarly caused GLUT4 translocation and glucose uptake in muscle during the fasting state *in vivo*. Intriguingly, expression of UBX-Cter caused depletion of PIST and mimicked insulin action to stimulate endoproteolysis of the endogenous TUG protein in muscle. The transgenic mice had increases in both whole-body glucose turnover and overall metabolic rate. Finally, aspects of this phenotype were maintained in the setting of high fat diet (HFD)-induced insulin resistance in mice. Together with previous work, our data support the idea that similar mechanisms control GLUT4 in muscle and adipose and identify a critical node for the control of whole-body glucose homeostasis.

EXPERIMENTAL PROCEDURES

Animals—Transgenic mTUG$^{\text{UBX-Cter}}$ mice were generated by cloning the cDNA sequence for a truncated murine TUG protein, UBX-Cter (residues 377–550), after a 1.3-kb segment derived from the mouse muscle creatine kinase promoter (−1256MCK-3Emut) (28, 29). This promoter (termed MCK^{3E}) contains specific mutations to drive expression in skeletal muscle but not in cardiac muscle or other tissues (30, 31). Following the coding sequence, a 2.2-kb segment of the human growth hormone gene was used to provide splice sites and polyadenylation and termination signals. The transgene was microinjected into SJL × C57BL/6 F2 fertilized oocytes, which were implanted in pseudopregnant females. Founder pups were identified by PCR of tail biopsies for a 171-bp segment of the human growth hormone sequence. Of 12 transgenic lines obtained, three were selected for further analysis. Preliminary analyses indicated that the phenotype was most robust in the line with greatest expression of the transgene, and this line was backcrossed at least 10 generations onto C57BL/6 (The Jackson Laboratory) and used in the heterozygous state for all analyses presented here. Male mice were used to avoid confounding effects of estrous cycles, and controls were age-matched, wild type mice (usually nontransgenic littermates). Mice were maintained in the Yale Animal Resources Center on a standard 12-h light/12-h dark cycle and were given *ad libitum* access to chow (Harlan-Teklad 2018, 5% calories from fat) and water unless otherwise stated. For studies using an HFD, mice were fed Harlan-Teklad TD93075 (55% calories from fat) for 3 weeks prior to experiments. The Institutional Animal Care and Use Committees at Yale University and the University of Michigan approved all procedures.

Tissue Analyses—For genotyping, DNA was extracted from ear punch or tail biopsies using a DNeasy kit (Qiagen). Both human growth hormone and transgene insertion site-specific primers were used for PCR. Tissues were collected from isoflurane-anesthetized mice after cervical dislocation, frozen in liquid N_2, and stored at −80 °C until further analysis. For blood glucose measurements, plasma was collected in EDTA and analyzed using a Beckman Glucose Analyzer II (Beckman Coulter). Plasma insulin was measured in duplicate using an ultrasensitive ELISA (ALPCO Diagnostics). Plasma lactate was measured in duplicate using a lactate kit (Trinity Biotech, Wicklow, Ireland). All other plasma and serum analyses were done on a Roche Applied Science COBAS Mira Plus automated chemistry analyzer. Tissue glycogen was determined using a glycogen assay kit (Biovision, Mountain View, CA).

Glucose Turnover Studies—To measure glucose turnover and uptake in the fasting state, we omitted the insulin infusion during our standard glucose-insulin clamp protocol (32, 33). Mice with an indwelling catheter in the right jugular vein were fasted overnight, and then 3-[^{3}H]glucose (PerkinElmer Life Sciences) was infused at 0.05 μCi/min for 120 min to determine basal glucose turnover. Next, to measure muscle-specific glucose uptake, 10 μCi of 2-deoxy-D-[1-^{14}C]glucose (PerkinElmer Life Sciences) was infused over 20 min. No insulin was infused, and care was taken to minimize the increase in plasma glucose, which would stimulate secretion of endogenous insulin. Blood samples were drawn by tail vein at 2, 5, 15, 25, 35, 45, and 55 min after the initiation of this 2-deoxy-D-glucose (2DOG) infusion. At study completion, mice were anesthetized with an intravenous pentobarbital sodium injection (150 mg/kg). Tissues were

harvested, snap frozen in liquid N_2 within 3 min of collection using liquid N_2-cooled tongs, and stored at −80 °C for subsequent analysis. Intracellular (6-phosphorylated) 2DOG was measured as described (34, 35). Glucose turnover and muscle-specific 2DOG uptake under maximal insulin stimulation were measured using hyperinsulinemic-euglycemic clamps as described (32, 35).

Body Composition, Metabolic Cages, and Necropsies—Body composition was determined using ^{1}H NMR (Bruker Minispec). To determine the weights of individual muscles or fat pads, mice were fasted for 6 h and sacrificed, and muscles were dissected, frozen in liquid N_2, and weighed (27). The comprehensive laboratory animal monitoring system (Columbus Instruments) was used to assess VO_2, VCO_2, energy expenditure, activity, and feeding during 48 h after an initial acclimatization period. Data are normalized to body weight, and 24-h averages are presented. Necropsies were done as described (36).

Quantitative Real Time PCR (Q-PCR) Analysis—Tissues were disrupted in TRIzol reagent (Invitrogen) using a Polytron homogenizer. Two micrograms of total RNA from each sample was treated with DNase I and reverse transcribed using Superscript III and random hexamer priming (Invitrogen). Q-PCR was performed using iQ SYBR Green Supermix on an iQ5 Cycler (Bio-Rad) or an Mx7500 system (Applied Biosystems). Samples were quantified using the standard curve method, normalized to endogenous 18 S RNA, and analyzed in duplicate with a tolerated variance of ~10%. Primer pairs were designed using Primer Express software (Applied Biosystems), and standard melt curves were done to confirm single PCR products. Primers for the TUG C terminus (within the transgene coding sequence) were CCTGACCCTGTATCCCTGGA and TCAGCCACTTGGGTACTTTGC, and 18 S control primers were TAGAGGGACAAGTGGCGTTC and CGCTGAGCCAGTCAGTGT. Primers for PIST were GTCCATGTTCCGATGGCTTGA and ATCTCGCCCAAAAGCAGATCC, which were used with 18 S control primers TTCCGATAACGAACGAGACTCT and TGGCTGAACGCCACTTGTC.

Insulin Stimulation, Immunoblotting, and Fractionation—Mice were fasted for 4–6 h or overnight as specified and then treated by intraperitoneal injection of insulin (8 units/kg) and glucose (1 g/kg) or an equivalent volume (0.3 ml) of phosphate-buffered saline. After 30 min, mice were anesthetized and sacrificed by cervical dislocation. Tissues were excised, snap frozen in liquid N_2, and stored at −80 °C. Tissues were homogenized in ice-cold radioimmune precipitation assay buffer (37) or in TRIzol reagent (Invitrogen), and immunoblots were done using Invitrogen NuPAGE or Tris acetate gels and buffers as described (12). In some instances, an SDS-PAGE Clean-up kit was used (GE Healthcare). Protein determinations were done using BCA or EZQ protein assays, and equal amounts of protein were loaded in each lane (12). Detection of proteins on immunoblots was done on film (by enhanced chemiluminescence) or using an Odyssey infrared imaging system (LI-COR Biosciences).

Isolation of T-tubule-enriched membrane fractions was done essentially as described (38). Similar results were obtained in replicate experiments using mice both with and without a GLUT4myc transgene (kindly provided by Dr. Amira Klip; Ref. 26). Briefly, mouse quadriceps muscles were homogenized in 1.5 ml of ice-cold Buffer A (20 mM $Na_4P_2O_7$, 20 mM Na_3PO_4, 1 mM $MgCl_2$, 0.3 M sucrose, 0.5 mM EDTA, 20 mM 2-iodocetamide) containing protease inhibitors (Roche Applied Science; two tablets/50 ml) using a Polytron tissue grinder. All steps were carried out at 4 °C. Samples were passed through a 23-gauge needle several times, and large aggregates were pelleted at 12,000 rpm for 1 min in a benchtop centrifuge. After saving a sample of the total protein, 700 μl was transferred to a new tube, diluted with an equal volume of Buffer A, and centrifuged at 12,000 rpm for 10 min. One milliliter of the supernatant was then centrifuged using a TLA 120.2 rotor (Beckman) at 18,000 rpm for 5 min. The pellet from this centrifugation was resuspended in 200 μl of Buffer A, and 500 μl of Buffer B (0.3 mM sucrose, 20 mM Tris, pH 7.0) was added. To strip myofibrillar proteins, 300 μl of 4 M KCl was added, and samples were incubated for 30–60 min at 4 °C with gentle mixing. Samples were then centrifuged at 57,000 rpm for 10 min at 4 °C in a TLA 120.2 rotor. The T-tubule-enriched membrane pellet was resuspended in 150 μl of Buffer B and analyzed by SDS-PAGE and immunoblotting. Quantification of individual proteins was done using a LI-COR Odyssey imaging system.

Antibodies used for immunoblotting include polyclonal antibodies directed to the C termini of TUG and GLUT4 (11, 12, 15). Monoclonal antibody 6H directed to the N terminus of the Na^+,K^+-ATPase α1 subunit was a gift from Dr. Michael Caplan (39). A polyclonal antibody directed to caveolin-1 was purchased from BD Transduction Laboratories (catalog number 610060; formerly C13630). A rabbit monoclonal anti-PIST antibody was from Abcam (catalog number ab109119). Antibodies to Golgin-160 and GCP60 were purchased from Santa Cruz Biotechnology (catalog numbers sc-292192 and sc-101277, respectively); Golgin-160 antisera were also raised to a 22-residue peptide corresponding to the N terminus of murine Golgin-160 (Covance Research Products). A β-actin loading control monoclonal antibody was from Pierce (catalog number MA5-15739).

Statistical Analysis—Data are presented as mean ± S.E. Significance was assessed using an unpaired, two-tailed *t* test or by two-way analysis of variance as appropriate (Prism, GraphPad Software). Differences were considered significant at $p < 0.05$.

RESULTS

The TUG protein is widely expressed and is required for efficient assembly of the Golgi complex (14). This general membrane trafficking pathway is adapted in a cell type-specific manner in which TUG undergoes insulin-stimulated endoproteolytic cleavage to control GLUT4 translocation (11, 15). In mice, global disruption of the gene encoding TUG may cause embryonic lethality, and no conditional knock-out model is presently available. Our previous work identified a truncated fragment of TUG that when expressed exogenously inhibits the function of endogenous, intact TUG to sequester GLUT4 within 3T3-L1 adipocytes (11, 12, 15). This artificial fragment, termed UBX-Cter, causes GLUT4 translocation and increases glucose uptake in cells not stimulated with insulin. The effects of UBX-Cter and RNAi-mediated TUG knockdown are indistinguishable in 3T3-L1 adipocytes; both mimic much of the full

effect of acute insulin stimulation on GLUT4 targeting and glucose uptake (11–13, 15). The UBX-Cter fragment is effective at very low abundance relative to intact TUG in 3T3-L1 adipocytes, suggesting that it turns over rapidly; it is hypothesized to act irreversibly to block the binding of intact TUG to Golgin-160, PIST, and associated Golgi matrix proteins (15). The endogenous TUG protein is then unable to trap GLUT4 at the Golgi matrix. To test the physiologic role of TUG to control GLUT4 targeting and glucose uptake in muscle, we generated transgenic mice in which UBX-Cter was expressed using a skeletal muscle-specific promoter (Fig. 1*A*). We predicted that these mice, termed $mTUG^{UBX\text{-}Cter}$ mice, would have increased cell surface GLUT4 and enhanced glucose uptake into muscle during the fasting state.

In muscles of $mTUG^{UBX\text{-}Cter}$ mice, the transgene mRNA was present at much greater abundance than endogenous TUG mRNA; however, the UBX-Cter protein was present at much lower abundance than endogenous TUG protein. Fig. 1*B* presents Q-PCR of an mRNA target encoding the TUG C terminus. Compared with endogenous TUG mRNA, the UBX-Cter transgene mRNA was highly expressed in quadriceps, gastrocnemius, and tibialis anterior; more modest expression was observed in soleus. No expression was detected in gonadal white adipose tissue, interscapular brown adipose tissue, heart, kidney, liver, or spleen. In gastrocnemius, despite 50–75-fold greater abundance of UBX-Cter mRNA compared with endogenous TUG mRNA, the UBX-Cter protein was one-fifth as abundant as endogenous, intact TUG protein (Fig. 1, *C* and *D*). We obtained similar results in tibialis anterior in which the UBX-Cter mRNA was ~40-fold more abundant than that of endogenous TUG mRNA (Fig. 1*B*) but in which UBX-Cter protein was present at ~14% of the abundance of endogenous, intact TUG protein (not shown). In gastrocnemius and tibialis anterior, there was no effect of the transgene on the abundance of intact TUG protein. These data support the prediction that UBX-Cter is an unstable protein that turns over rapidly. As discussed below, transgene mRNA abundance correlated with its efficacy to disrupt intact TUG action in various muscles. If this efficacy was limited, the whole-body phenotype of the transgenic mice may have been minimized. For tissue-specific analyses, we focused on quadriceps, gastrocnemius, and tibialis anterior, which had the highest levels of transgene mRNA expression.

The UBX-Cter fragment is thought to act by an irreversible mechanism to block intracellular GLUT4 sequestration (15). In 3T3-L1 adipocytes, this fragment is effective at very low abundance such that it is practically undetectable on immunoblots, and it contains potential degradation signals, including a ubiquitin-like domain and PEST sequence (40). Therefore, we considered that UBX-Cter may cause degradation of an interacting protein together with itself. Candidate UBX-Cter-interacting proteins include PIST and Golgin-160 (15, 41) as well as the Golgin-160-binding protein, GCP60 (42, 43). Of these, PIST was selectively depleted in quadriceps muscles of transgenic mice compared with controls (Fig. 1*E*). We confirmed that PIST is also depleted in 3T3-L1 adipocytes containing the UBX-Cter fragment (not shown). Abundance of the mRNA encoding PIST was unaffected in quadriceps muscle (Fig. 1*F*). The data are consistent with the idea that UBX-Cter reduces PIST protein stability likely by recruiting enzymes that mediate ubiquitylation and proteasomal degradation.

There are two ways in which UBX-Cter-induced depletion of PIST may redistribute GLUT4 from its sequestration compartment to the cell surface. One possibility is that PIST depletion removes an essential component of an "anchoring" site to which TUG links GSVs in unstimulated cells. Similar to TUG RNAi, the ability of TUG to trap GLUT4 intracellularly would then be compromised so that GLUT4 is redirected to the plasma membrane (12, 13). A second possibility is that PIST depletion releases the GSVs by causing TUG endoproteolytic cleavage. This would be similar to acute insulin action, which is mediated by a signal through TC10α to PIST to TUG (3, 15). These two mechanisms are not necessarily exclusive of each other. However, the second mechanism is compatible with the possibility that proteins other than PIST (*e.g.* Golgin-160 and GCP60) may serve as anchors to which TUG links GLUT4 in unstimulated cells. We have found that GCP60 in particular binds the TUG C-terminal peptide and is required for GLUT4 intracellular retention.[4] Therefore, we favored the idea that endogenous TUG undergoes constitutive endoproteolytic cleavage not regulated by insulin in muscles containing the UBX-Cter transgene.

Accordingly, we examined whether insulin stimulates acute, endoproteolytic cleavage of TUG in control quadriceps muscles and tested the effect of the UBX-Cter transgene on this processing. We treated fasting mice by intraperitoneal injection of insulin and glucose or saline control, then sacrificed the mice, and immunoblotted muscle lysates. Insulin stimulated the conversion of intact 60-kDa TUG into its 42-kDa C-terminal cleavage product in wild type mice (Fig. 1*G*). In $mTUG^{UBX\text{-}Cter}$ transgenic mice, the cleavage product was observed in saline-treated animals, and there was no further effect of insulin to stimulate conversion of intact TUG into its C-terminal product. The presence of multiple bands at ~42 kDa may be due to degradation of this cleavage product, which is moderately short lived (15). Data from several animals were quantified in Fig. 1*H*, which plots the ratio of the 42-kDa cleavage product to total (*i.e.* 60- + 42-kDa) TUG proteins. The abundance of intact TUG was variably decreased in transgenic and in insulin-stimulated wild type control muscles compared with unstimulated control muscles, and the ratio of products to total TUG proteins was a more sensitive and consistent readout of insulin action. The UBX-Cter protein was present at very low abundance, suggesting that it may turn over more rapidly in quadriceps than in other muscles. We conclude that insulin stimulates TUG cleavage in muscle. Furthermore, the truncated TUG UBX-Cter protein promotes endoproteolytic cleavage of endogenous, intact TUG in the absence of insulin stimulation, thus preventing the entrapment of GLUT4 at the Golgi matrix.

The data imply that the UBX-Cter fragment acts in a highly specific manner to stimulate a particular insulin action. TUG is cleaved between residues 164 and 165 likely by a thiol-type

[4] J. P. Belman and J. S. Bogan, unpublished data.

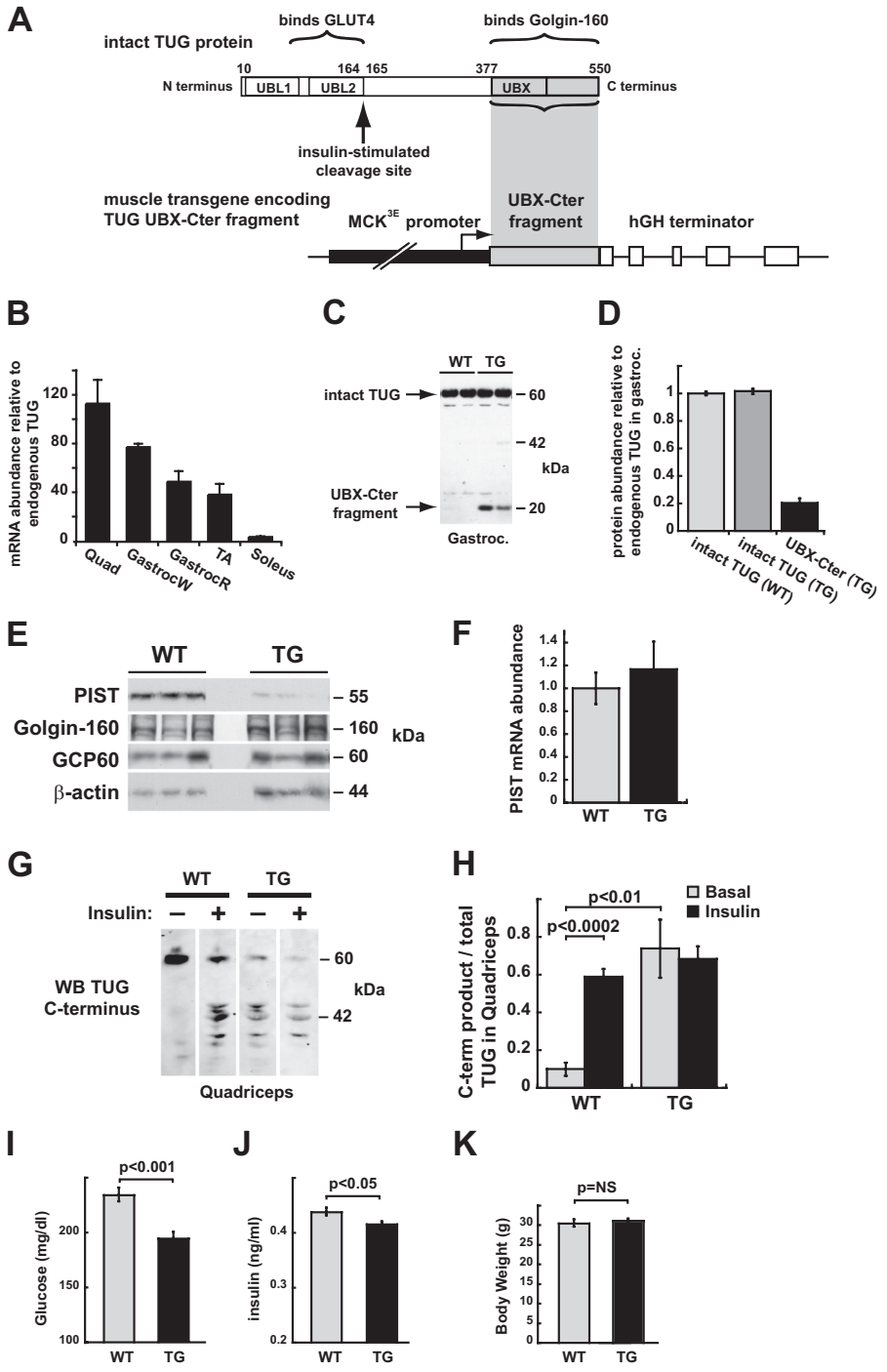

FIGURE 1. **mTUG$^{UBX\text{-}Cter}$ mice have depletion of PIST and constitutive endoproteolysis of TUG in muscle and reduced fasting glucose and insulin concentrations.** *A*, mTUG$^{UBX\text{-}Cter}$ mice contain a transgene for skeletal muscle-specific expression of a TUG fragment, UBX-Cter, which corresponds to residues 377–550 of intact TUG protein, as diagrammed. This fragment contains a ubiquitin-like UBX domain and binds Golgin-160 and associated proteins at the Golgi matrix but not GLUT4 or other proteins in GLUT4 storage vesicles. *hGH*, human growth hormone. *B*, Q-PCR was used to measure the relative abundances of UBX-Cter mRNA in quadriceps (*Quad*), white gastrocnemius (*GastrocW*), red gastrocnemius (*GastrocR*), tibialis anterior (*TA*), and soleus of mTUG$^{UBX\text{-}Cter}$ mice compared with that of endogenous TUG mRNA in wild type control tissues. *C*, mixed gastrocnemius (*Gastroc.*) lysates from mTUG$^{UBX\text{-}Cter}$ TG and control (WT) mice were immunoblotted using an antibody to the TUG C terminus. *D*, relative abundances of intact TUG and truncated TUG UBX-Cter proteins in gastrocnemius were quantified and plotted. Data are presented as mean ± S.E.; $n = 7$ in each group. *E*, mixed hind limb muscle lysates from WT and TG mice were immunoblotted to detect the indicated proteins. *F*, Q-PCR was used to measure the relative abundance of PIST mRNA in quadriceps of WT and TG mice. Data are presented as mean ± S.E.; $n = 5$ in each group. *G*, TUG endoproteolytic processing was assayed by immunoblotting quadriceps of WT and TG mice. Fasted animals were treated by intraperitoneal injection of saline or insulin-glucose solution and sacrificed after 30 min. Quadriceps muscle lysates were immunoblotted to detect intact TUG (60 kDa) and C-terminal cleavage products (~42 kDa). *H*, the ratio of the C-terminal (*C-term*) cleavage products (~42 kDa) to total TUG proteins (60 + ~42 kDa) was quantified. Data are presented as mean ± S.E.; $n = 3$–4 mice in each group. *I–K*, plasma glucose, plasma insulin, and body weight were measured in 20-week-old mice fasted for 4 h. Data are presented as mean ± S.E.; $n = 6$ in each group. *Error bars* represent S.E. *WB*, Western blot; *NS*, not significant.

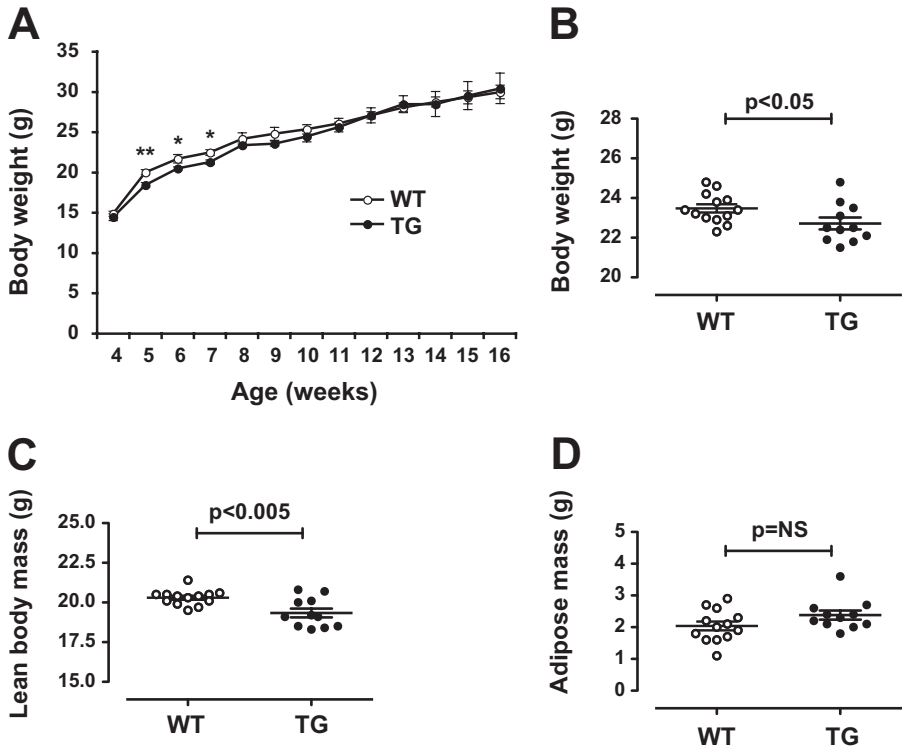

FIGURE 2. **Weight and body composition of mTUG$^{UBX\text{-}Cter}$ mice.** *A*, total body weights of mTUG$^{UBX\text{-}Cter}$ and control mice are plotted as a function of age. *, $p < 0.05$; **, $p < 0.01$ ($n = 7$ in each group). *B–D*, body weight, lean body mass, and fat mass were measured in a larger cohort of 12-week-old mice used for studies of glucose turnover during fasting. Data are presented as mean ± S.E.; $n = 9–13$ in each group. *Error bars* represent S.E. *NS*, not significant.

deubiquitylating enzyme family member (15). Cleavage is activated upon receipt of an insulin signal transduced from the TC10α GTPase to PIST to TUG. The data support a model in which PIST inhibits TUG proteolysis in the absence of GTP-bound TC10α. By causing the degradation of PIST together with itself, UBX-Cter removes this negative regulator and permits access of the protease to the cleavage site. Insulin likely acts by a similar mechanism in which GTP-TC10α causes the displacement of PIST from TUG to permit activity of the TUG protease. This model fits well with the concept that UBX-Cter acts irreversibly. The effect of insulin to stimulate TUG cleavage in skeletal muscle was more dramatic than that observed in 3T3-L1 adipocytes (15). Cultured 3T3-L1 cells are an imperfect model system and, as insulin-stimulated cleavage is differentiation-dependent, cleavage products are often observed in unstimulated cells. Thus, it is not surprising that the effect of UBX-Cter to promote TUG cleavage was not detected in previous work using 3T3-L1 cells. The main points are that insulin stimulates TUG cleavage in muscle and that UBX-Cter also stimulates this specific insulin action in fasting mTUG$^{UBX\text{-}Cter}$ transgenic mice.

We predicted that fasting mTUG$^{UBX\text{-}Cter}$ mice would have GLUT4 translocation and increased glucose uptake into muscle and consequently reduced plasma glucose and insulin concentrations. Supporting this prediction, 20-week-old mTUG$^{UBX\text{-}Cter}$ mice had significantly reduced fasting plasma glucose and insulin concentrations compared with wild type controls (Fig. 1, *I* and *J*). These effects were not attributable to altered body weight (Fig. 1*K*). Immunoblots showed that GLUT4 and GLUT1 abundances were unchanged in various muscles; in some experiments, quadriceps GLUT4 abundance was slightly reduced (see below). These data are consistent with the hypothesis that during the fasting state GLUT4 translocation in mTUG$^{UBX\text{-}Cter}$ mice results in increased glucose uptake in muscle, reduced plasma glucose concentrations, and consequently reduced insulin concentrations.

To characterize the growth and body composition of mTUG$^{UBX\text{-}Cter}$ mice, we measured their body weights at various ages. As shown in Fig. 2*A*, mTUG$^{UBX\text{-}Cter}$ mice had reduced weights at 5–7 weeks that subsequently converged with weights of control mice. When a greater number of mice were analyzed for glucose turnover studies below, a slight (~3%) reduction in body weight remained significant at 12 weeks of age (Fig. 2*B*). In this group, the transgenic mice had ~5% reduced lean body mass and a trend toward increased fat mass (Fig. 2, *C* and *D*). We confirmed that the masses of individual quadriceps, tibialis anterior, extensor digitorum longus, and epitrochlearis muscles were reduced in 17-week-old mTUG$^{UBX\text{-}Cter}$ mice compared with controls (not shown). There was a trend toward increased gonadal white adipose tissue mass in transgenic mice compared with controls both in absolute terms and relative to total body weight; however, this did not reach statistical significance (not shown). Overall, the main finding was slightly reduced lean body mass.

Analysis of blood from fasting 12-week-old mice again demonstrated reduced plasma glucose in mTUG$^{UBX\text{-}Cter}$ transgenic mice compared with controls (Table 1). Electrolytes and blood urea nitrogen were unchanged. A lipid profile revealed that mTUG$^{UBX\text{-}Cter}$ mice have reduced triglycerides, total cholesterol, and HDL cholesterol compared with controls. LDL cho-

TABLE 1
Fasting blood analyses

Measurements were done on plasma of 12-week-old WT and mTUG$^{UBX\text{-}Cter}$ TG mice fasted for 4–6 h. Data are means ±S.E.; $n = 8–9$ in each group. NEFA, nonesterified fatty acids; BUN, blood urea nitrogen.

Parameter	WT	TG
Glucose (mg/dl)	171 ± 13	126 ± 14[a]
Sodium (mg/dl)	138.5 ± 2.1	139.9 ± 1.6
Chloride (mg/dl)	119.5 ± 1.1	117.8 ± 0.8
Potassium (mg/dl)	4.6 ± 0.1	4.7 ± 0.2
BUN (mg/dl)	21.1 ± 1.7	22.7 ± 1.0
Lipid profile		
Triglycerides (mg/dl)	61.2 ± 1.4	47.9 ± 4.4[a]
Total cholesterol (mg/dl)	109.0 ± 1.7	90.5 ± 8.9[a]
HDL cholesterol (mg/dl)	68.1 ± 3.8	42.8 ± 4.4[a]
LDL cholesterol (mg/dl)	2.9 ± 0.4	2.9 ± 0.6
NEFA (mg/dl)	1.4 ± 0.2	1.1 ± 0.1

[a] $p < 0.05$.

lesterol and nonesterified fatty acids were unchanged. Necropsies of 20-week-old animals revealed no gross or histological differences between transgenic and wild type control mice in any of the tissues examined.

To measure fasting whole-body glucose turnover and muscle-specific uptake *in vivo* in conscious mice, we used a study protocol consisting of a 2-h basal glucose turnover period followed by a 1-h 2DOG uptake period. In contrast to the observed reductions in plasma glucose concentrations following a 4–6-h fast, there were no differences in plasma glucose concentrations following a 14-h overnight fast (Fig. 3*A*). This is consistent with data showing that glycemia after a 6-h fast is a better indicator of insulin sensitivity in mice compared with glycemia after an overnight fast (44). Insulin measurements on the samples from the overnight fasted mice showed that compared with wild type controls transgenic mice had significantly reduced fasting plasma insulin concentrations (Fig. 3*B*). Basal glucose turnover was increased by 17% in mTUG$^{UBX\text{-}Cter}$ mice and was 12.1 ± 0.6 *versus* 10.3 ± 0.3 mg/(kg-min) in transgenic *versus* control mice (Fig. 3*C*). To avoid the potential that the slight decrease in body mass may have accounted for the increased whole-body glucose turnover rates normalized per kg of body weight, we normalized these data per mouse. As shown in Fig. 3*D*, basal glucose turnover was increased by 14% in transgenic *versus* control animals when analyzed on a per mouse basis (Fig. 3*D*). This robust increase supports the idea that TUG function in muscle regulates whole-body glucose turnover during the fasting state. We also observed a 15% increase in glycolysis in mTUG$^{UBX\text{-}Cter}$ mice compared with controls during the study (Fig. 3*E*). In quadriceps muscles, *in vivo* 2DOG uptake was increased by 2.7-fold in transgenic *versus* control mice (Fig. 3*F*). We conclude that muscle-specific activation of TUG cleavage results in markedly enhanced muscle glucose uptake in fasting mice. Moreover, the increase in muscle glucose uptake accounts for the increased basal rate of glucose production.

We hypothesized that the UBX-Cter protein would not affect glucose turnover or muscle 2DOG uptake in hyperinsulinemic-euglycemic clamp experiments. This prediction was based on two lines of reasoning. First, previous data support the idea that during sustained, maximal insulin exposure, GLUT4 recycles to the cell surface directly from endosomes and bypasses a TUG-regulated compartment (13). Thus, TUG acts only in unstimulated cells and upon cleavage to mediate the acute release of sequestered GLUT4 into a cell surface recycling pathway. Second, data above show that the UBX-Cter protein caused cleavage of intact TUG in unstimulated quadriceps muscles, mimicking acute insulin action (Fig. 1, *G* and *H*). There was no further biochemical effect of the transgene in samples of insulin-stimulated muscles. Consistent with these considerations, we observed similar glucose infusion rates in control and mTUG$^{UBX\text{-}Cter}$ mice in hyperinsulinemic-euglycemic clamp studies (not shown). Whole-body glucose turnover and quadriceps muscle-specific glucose uptake were no different in transgenic and control mice (Fig. 3, *G* and *H*). These data support the idea that effects of the UBX-Cter protein are specific to the fasted, low insulin state.

Of note, quadriceps-specific 2DOG uptake in fasting mice was 83.7 ± 18 nmol/(g-min) in transgenic mice and 31.5 ± 6.5 nmol/(g-min) in wild type controls (Fig. 3*F*), and uptake in hyperinsulinemic-euglycemic clamp studies was 98.5 ± 19.4 nmol/(g-min) in transgenic mice and 78.2 ± 12.6 nmol/(g-min) in wild type controls (Fig. 3*H*). Plasma glucose concentrations were similar in fasting and clamped mice. Thus, effects of the transgene and of insulin to increase quadriceps-specific 2DOG uptake were similar in magnitude. Insulin had a much greater effect to increase whole-body glucose disposal, and the turnover rates measured in the hyperinsulinemic clamp studies (Fig. 3*G*) were much greater than those in either wild type (WT) or transgenic (TG) mice during fasting (Fig. 3*C*). These data are consistent with the idea that effects of the transgene were limited in muscles with lower transgene mRNA expression and in adipose where transgene expression was undetectable. Together with data below, the quadriceps-specific 2DOG uptake data support the idea that the action of insulin to cleave TUG can account for the bulk of its overall effect to stimulate glucose uptake in muscle.

We next tested whether mTUG$^{UBX\text{-}Cter}$ mice have increased muscle glycogen content, which would further support the idea that muscle glucose uptake is increased. Fig. 4*A* shows that compared with controls transgenic mice fasted 4–6 h had increased glycogen in quadriceps, gastrocnemius, and tibialis anterior, which had greater expression of the transgene, and not in soleus, which had lower expression. No increase in glycogen content was observed in liver or gonadal fat in which expression of the UBX-Cter transgene was undetectable. The correlation of UBX-Cter transgene mRNA abundance and muscle glycogen content supports the idea that that the transgene enhances glucose uptake by a direct, cell-autonomous effect and not by indirect systemic effects.

Table 2 further correlates UBX-Cter mRNA abundance and functional effects. In addition to increased glycogen content, increased basal TUG cleavage and 2DOG uptake were observed in quadriceps where UBX-Cter mRNA abundance was greatest. In gastrocnemius and tibialis anterior, we observed only increased glycogen content, which is likely a more sensitive indicator of glucose uptake than the 2DOG measurement. In soleus, where UBX-Cter mRNA abundance was much lower, none of these effects were observed. The correlation of UBX-

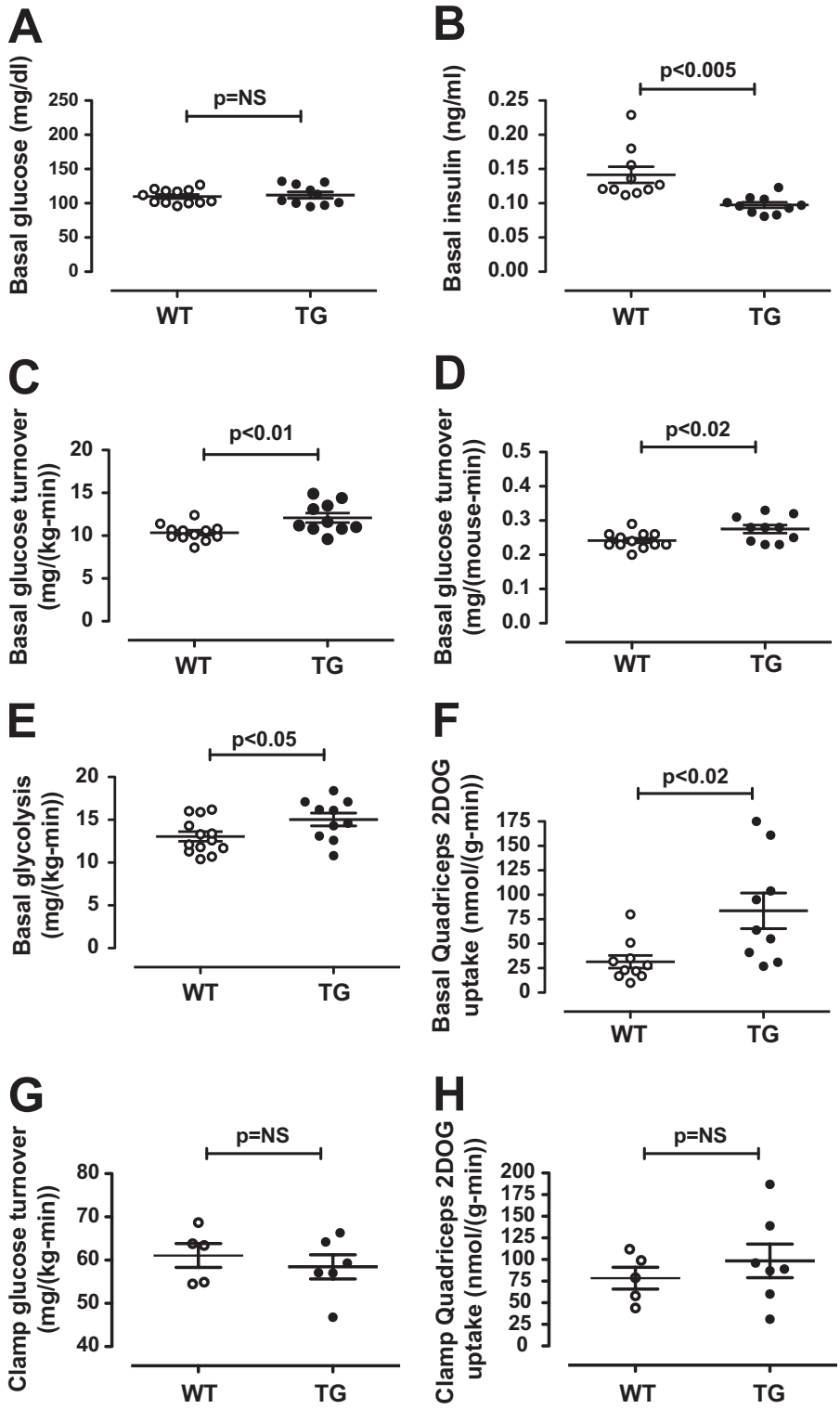

FIGURE 3. **mTUG$^{UBX\text{-}Cter}$ mice have increased whole-body glucose turnover and muscle-specific glucose uptake during fasting but not during hyperinsulinemic clamp studies.** *A–F*, 12-week-old mTUG$^{UBX\text{-}Cter}$ TG and control (WT) mice were fasted overnight, and then [^{3}H]glucose was infused over 2 h to measure basal glucose turnover. Next, to measure uptake, ^{14}C-labeled 2DOG was infused over 20 min, and the study was terminated at the 3-h time point. No insulin was infused. Basal plasma glucose and insulin concentrations (*A* and *B*) and glucose turnover per body weight (*C*) and per mouse (*D*) are plotted. *E*, glycolysis during the entire study, including both the basal and uptake periods, is plotted. *F*, uptake of 2DOG into quadriceps muscles was measured and plotted. Data are presented as mean ± S.E.; $n = 9–13$ in each group. *G* and *H*, hyperinsulinemic-euglycemic clamp studies were performed in 14-week-old WT and TG mice. Plasma glucose concentrations were identical to those in fasting mice (*A*) and were maintained during the study. *G*, whole-body glucose turnover was determined and plotted. *H*, quadriceps muscle-specific 2-deoxyglucose uptake was measured and plotted. Data are presented as mean ± S.E.; $n = 5$ WT and 6 TG mice. *Error bars* represent S.E. *NS*, not significant.

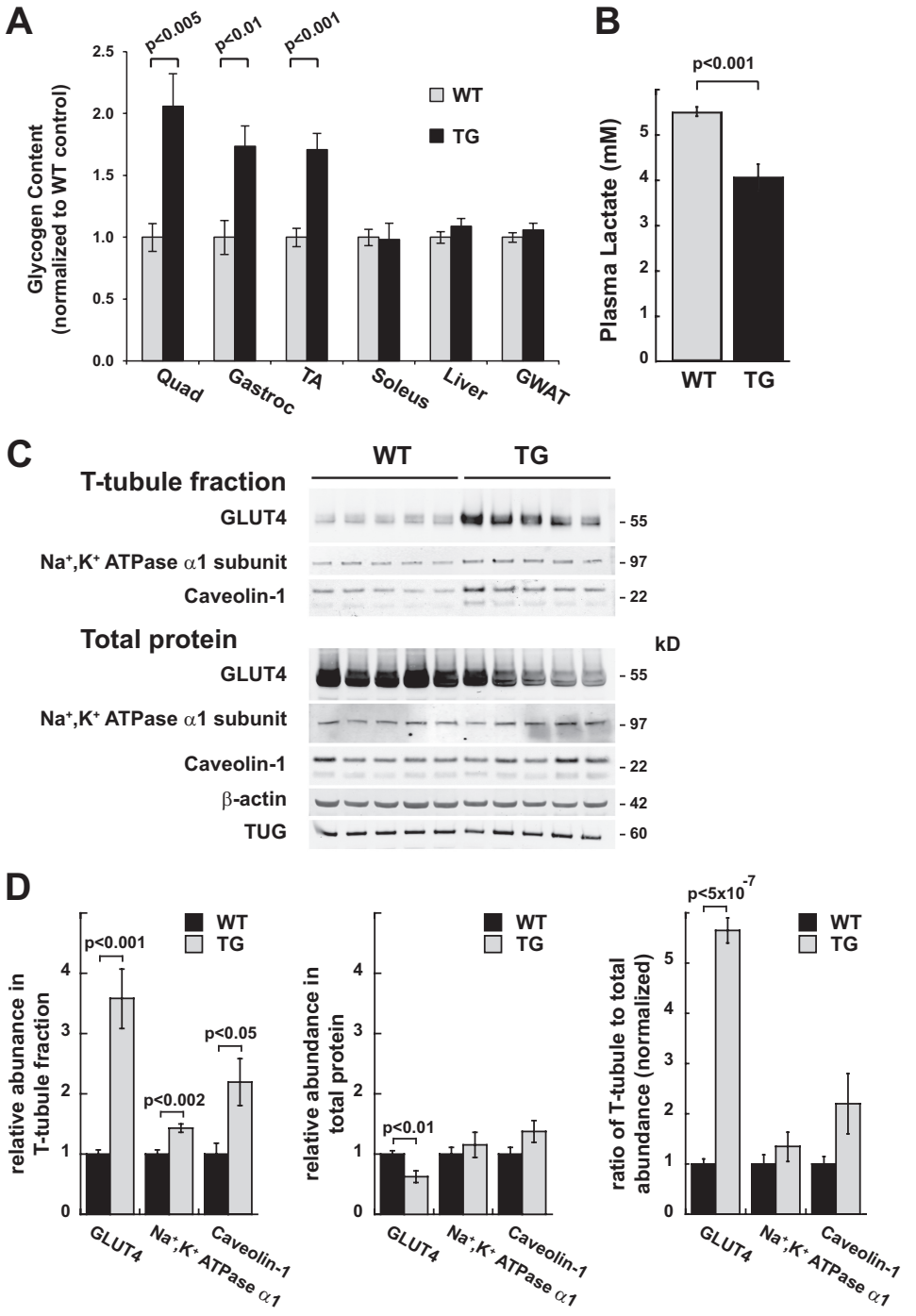

FIGURE 4. **Increased muscle glycogen, reduced plasma lactate, and targeting of GLUT4 to T-tubules in fasting mTUG$^{UBX\text{-}Cter}$ mice.** Control (WT) and mTUG$^{UBX\text{-}Cter}$ TG mice were fasted for 4–6 h and then sacrificed. *A*, glycogen content was measured, normalized to protein concentration in each of the indicated tissues, and plotted. *B*, plasma lactate was measured in WT and TG mice and plotted. *C* and *D*, T-tubule-enriched membrane fractions and total protein homogenates of quadriceps muscles from WT and TG mice were immunoblotted as indicated (*C*), and quantification of protein abundances and targeting to the T-tubule fraction is plotted (*D*). Data are presented as mean ± S.E.; $n = 5$ in each group. *Error bars* represent S.E. *Quad*, quadriceps; *Gastroc*, gastrocnemius; *TA*, tibialis anterior; *GWAT*, gonadal white adipose tissue.

Cter expression with these biological effects is strong evidence that the UBX-Cter acts only partially in a subset of muscles to disrupt the action of intact TUG to sequester GLUT4. It was surprising that UBX-Cter had such limited efficacy in skeletal muscle because it is very effective at redistributing GLUT4 in 3T3-L1 adipocytes (12). Possibly, this may be related to acetylation of residues at the C terminus of TUG and of UBX-Cter, which is greater in 3T3-L1 adipocytes than in muscle and which is required for the C-terminal peptide to bind GCP60.[4] If this binding enhances UBX-Cter incorporation into a complex containing PIST, then it may promote PIST degradation. Regardless, the data support the idea that the whole-body phenotype of mTUG$^{UBX\text{-}Cter}$ mice was limited due to incomplete or absent effects of the transgene in some muscles.

TABLE 2

Correlation of UBX-Cter mRNA abundance and effects

UBX-Cter mRNA abundances are given relative to endogenous TUG mRNA abundances in the identical tissues of wild type mice (as plotted in Fig. 1*B*). Cleavage indicates the abundance ratio of the 42-kDa cleavage product to total (*i.e.* 60- + 42-kDa) TUG proteins (as in Fig. 1*H*). 2DOG uptake is the ratio of fasting, tissue-specific 2-deoxyglucose uptake in transgenic *versus* wild type control muscles, which was significant in quadriceps ($p < 0.02$; Fig. 3*F*) but not in other muscles. Glycogen is normalized per mg of protein in each muscle and is given as the increase relative to that in wild type control muscles (Fig. 4*A*). Gastroc., gastrocnemius; TA, tibialis anterior; ND, not done; NS, not significant.

	Quadriceps	Gastroc.	TA	Soleus
UBX-Cter mRNA	112 ± 29	70 ± 9	39 ± 16	3 ± 0.6
Cleavage (product/total)	0.73 ± 0.15	~0.01 (NS)	~0.01 (NS)	ND
2DOG uptake (-fold increase in TG *vs.* WT)	2.7	1.2 (NS)	1.1 (NS)	ND
Glycogen (-fold increase in TG *vs.* WT)	2.1 ± 0.3	1.7 ± 0.2	1.7 ± 0.1	1.0 ± 0.1 (NS)

Circulating lactate concentrations were reduced in $mTUG^{UBX\text{-}Cter}$ transgenic mice compared with wild type controls (Fig. 4*B*). This result suggests that in addition to being stored as glycogen the increased glucose that is taken up in the transgenic mice is oxidized or that lactate is more rapidly utilized by hepatic gluconeogenesis. These possibilities are not exclusive. Both effects would be compatible with the increased metabolic rate we observed in the data below.

To show biochemically that GLUT4 is targeted to the cell surface in fasting $mTUG^{UBX\text{-}Cter}$ mice, we immunoblotted T-tubule-enriched and total membrane fractions from quadriceps muscles. In transgenic mice compared with controls, GLUT4 abundance was increased 3.6-fold in the T-tubule-enriched membranes, and it was decreased by 37% in total protein homogenates (Fig. 4, *C* and *D*). These data are consistent with previous results showing that TUG sequesters GLUT4 away from degradative pathways as well as from the plasma membrane (9, 12). The absolute increase in T-tubule GLUT4 abundance is similar to the 2.7-fold increase in *in vivo* 2DOG uptake (Fig. 3*F*), supporting the idea that the T-tubule fractions are reasonably pure. Overall, the proportion of GLUT4 that was present in T-tubules was increased 5.7-fold in the transgenic mice compared with controls (Fig. 4*D*). We also immunoblotted the α1 subunit of the Na^+,K^+-ATPase and caveolin-1. In transgenic mice, the abundances of these proteins were increased in T-tubule fractions. However, there was also a trend toward increased abundances of these proteins in the total membrane fractions. As a result, the proportions of these proteins that were distributed to T-tubules were not significantly different in $mTUG^{UBX\text{-}Cter}$ mice *versus* wild type controls. These data support the idea that TUG acts in a specific manner to regulate GLUT4 targeting in muscle similar to adipocytes (11–13, 15).

To study how disruption of TUG regulation in muscle alters metabolic rate, we measured VO_2, VCO_2, and energy expenditure. Fig. 5, *A–F*, shows that compared with nontransgenic controls $mTUG^{UBX\text{-}Cter}$ mice had 12–13% increases in all three of these parameters. These increases were observed throughout the light-dark cycle, and 24-h averaged data revealed highly significant differences by genotype. These differences were not attributable to increased locomotor activity (Fig. 5*G*). The respiratory exchange ratio (RER) was not different in $mTUG^{UBX\text{-}Cter}$ mice and controls, although it is possible that subtle alterations in fuel substrate are not reflected in these measurements (Fig. 5*H*). Finally, there was a trend toward increased food consumption in $mTUG^{UBX\text{-}Cter}$ mice that did not reach statistical significance (Fig. 5*I*). We conclude that disruption of TUG action in muscle by the UBX-Cter transgene results in an increased metabolic rate.

To study the phenotype of $mTUG^{UBX\text{-}Cter}$ mice in the setting of diet-induced insulin resistance, we placed transgenic and wild type control mice on an HFD (55% calories from fat) for 3 weeks. Previous hyperinsulinemic-euglycemic clamp studies show that this intervention impairs skeletal muscle-specific glucose uptake by ~40% (31, 35, 45, 46). After HFD feeding, 12-week-old $mTUG^{UBX\text{-}Cter}$ and control mice had no differences in body weight or fat mass by genotype (not shown). We measured whole-body glucose turnover during the fasting state as in Fig. 3 above. In contrast to chow-fed mice, HFD-fed $mTUG^{UBX\text{-}Cter}$ mice had markedly decreased plasma glucose concentrations after a 14-h fast compared with HFD-fed wild type controls (Fig. 6*A*). Basal glucose turnover was not significantly different and was not increased in HFD-fed $mTUG^{UBX\text{-}Cter}$ *versus* control mice (Fig. 6*B*). Indeed, if a potential outlier in the control group is excluded, turnover would actually be decreased in the transgenic mice compared with controls. We considered that glucose turnover may have been reduced by the lower plasma glucose concentrations in transgenic animals and so calculated glucose clearance. As shown in Fig. 6*C*, basal glucose clearance was not different in $mTUG^{UBX\text{-}Cter}$ and control mice. Finally, we observed no difference in quadriceps-specific, fasting 2DOG uptake in HFD-fed transgenic *versus* control mice (not shown). We conclude that compared with transgenic mice fed regular chow transgenic mice fed the HFD had a greater reduction in fasting glucose but no increase in glucose turnover compared with wild type controls on the same diet. Possibly, glucose turnover was limited by hepatic glucose output so that reduced fasting plasma glucose concentrations were the main observation in transgenic mice fed an HFD.

Hyperinsulinemic-euglycemic clamp studies of the HFD-fed mice revealed no differences in whole-body insulin-stimulated glucose turnover in control and $mTUG^{UBX\text{-}Cter}$ transgenic mice. This result was similar to that in transgenic mice on regular chow described above and was not unexpected. In HFD-fed transgenic and control mice, whole-body glucose turnover rates were 32.4 ± 1.6 and 32.4 ± 2.6 mg/(g-min), respectively. By comparison, chow-fed transgenic and control mice had turnover rates of 58.5 ± 2.8 and 61.1 ± 2.8 mg/(g-min), respectively (Fig. 3*G* above). These data confirm that the HFD resulted in whole-body insulin resistance and are consistent with the idea that intact TUG acts primarily in the fasting, low insulin state.

To study the effects of TUG disruption on the metabolic rate in the setting of HFD-induced insulin resistance, we placed

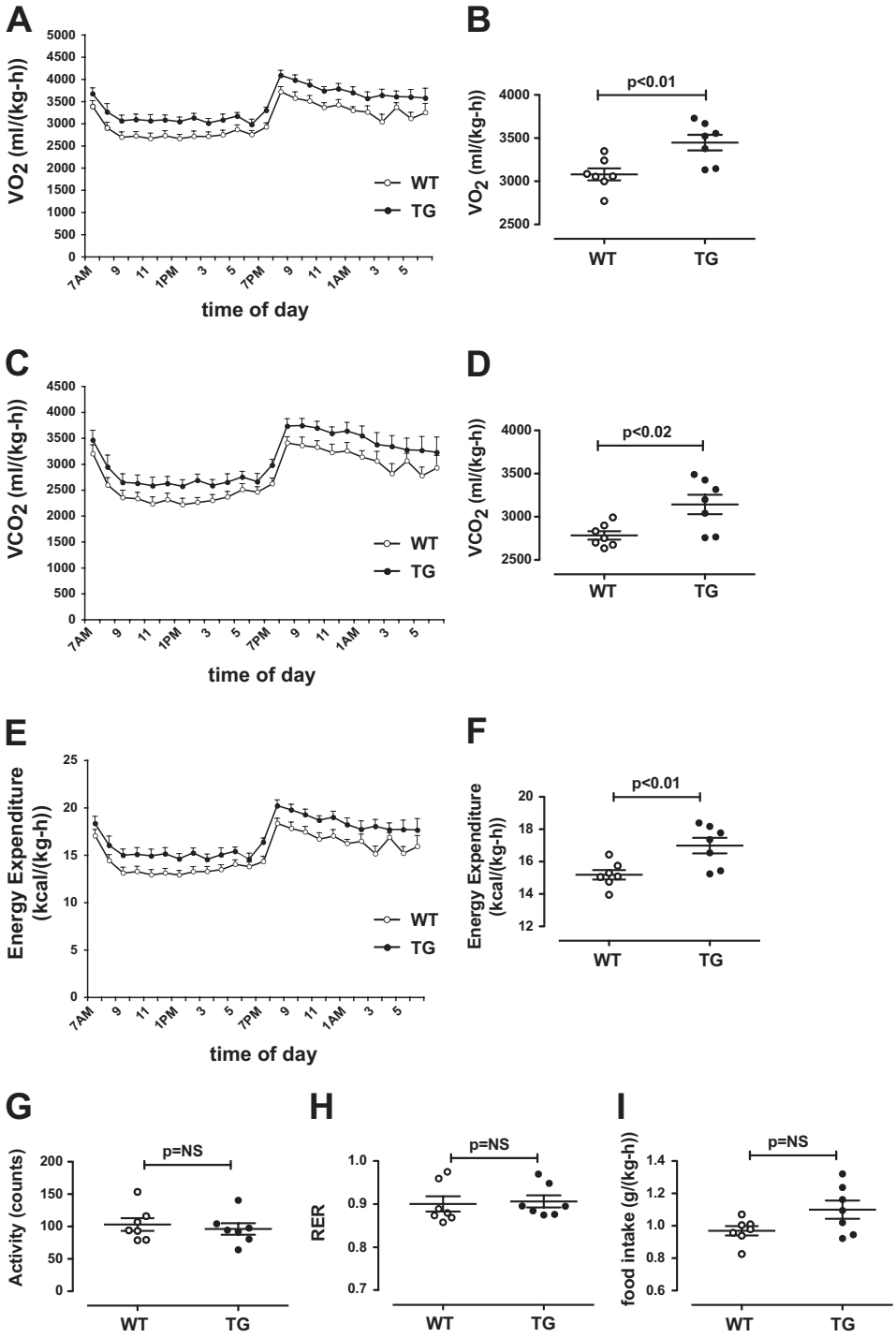

FIGURE 5. **Increased metabolic rate in mTUG$^{UBX\text{-}Cter}$ mice.** Energy metabolism was analyzed in 12-week-old control (WT) and mTUG$^{UBX\text{-}Cter}$ TG mice maintained on a 12-h light/12-h dark cycle with a darkened room from 7:00 pm to 7:00 am. *A–D*, VO_2 and VCO_2 were measured and plotted with respect to clock time (*A* and *C*) and as 24-h averages (*B* and *D*). *E* and *F*, energy expenditure was measured by indirect calorimetry and plotted with respect to clock time (*E*) and as a 24-h average (*F*). *G–I*, locomotor activity (beam breaks), averaged RER, and food consumption are plotted. Data are presented as mean ± S.E.; $n = 7$ in each group. *Error bars* represent S.E. *NS*, not significant.

14-week-old transgenic and control mice in metabolic cages. Similar to regular chow-fed animals, mTUG$^{UBX\text{-}Cter}$ mice had a ~9% increase in VO_2, VCO_2, and energy expenditure (Fig. 7, *A–F*). These differences were not attributable to increased locomotor activity (Fig. 7*G*). Indeed, the increases in VO_2, VCO_2, and energy expenditure were all greater during daylight hours when mice were less active than during the night. This is again consistent with the hypothesis that the transgene modulates metabolism during the fasting state. Fig. 7*H* shows that RER was appropriately decreased in HFD-fed mTUG$^{UBX\text{-}Cter}$ and wild type mice compared with chow-fed animals (compare Fig. 5*H*); there was no difference in RER between genotypes. Of note, the mTUG$^{UBX\text{-}Cter}$ mice had a 14% increase in food consumption (Fig. 7*I*) but without any increase in total body

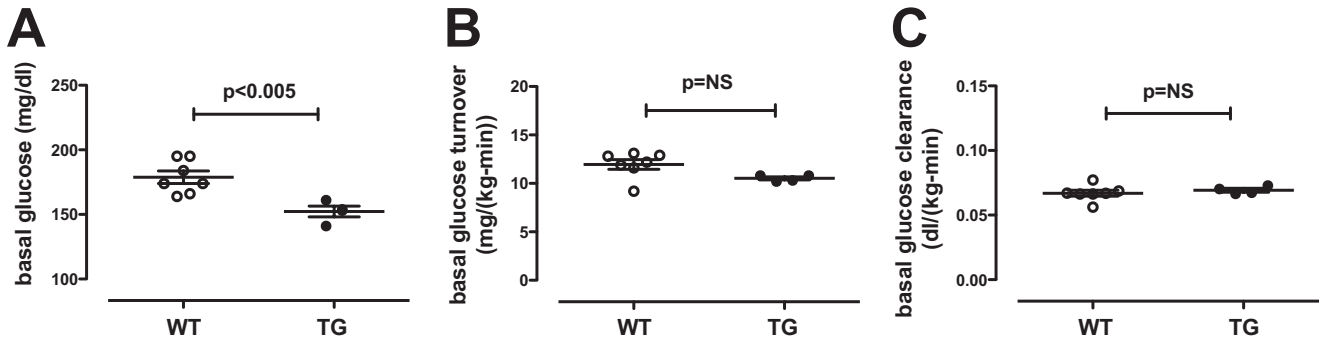

FIGURE 6. **Reduced fasting plasma glucose in HFD-fed mTUG$^{UBX\text{-}Cter}$ mice.** 13-week-old HFD-fed mTUG$^{UBX\text{-}Cter}$ TG and control (WT) mice were fasted overnight, and then basal glucose turnover studies were performed without insulin infusion. *A*, fasting plasma glucose concentrations are plotted. *B*, basal whole-body glucose turnover was measured and plotted. *C*, basal plasma glucose clearance is plotted. Data are presented as mean ± S.E.; $n = 7$ WT and 4 TG mice. *Error bars* represent S.E. *NS*, not significant.

weight, fat mass, or percent fat mass (Fig. 7, *J–L*). This may represent a compensatory increase in food intake that prevented a decrease in body weight. We conclude that disruption of TUG action in muscle by the UBX-Cter transgene results in an increased metabolic rate in HFD-fed, insulin-resistant mice.

DISCUSSION

The identification of the main trafficking steps at which insulin acts to control GLUT4 translocation has been a longstanding puzzle. Our data show *in vivo* in skeletal muscle that a TUG-regulated step is a major point of control for GLUT4 trafficking and glucose uptake. We observed a ~5.7-fold increase in the fraction of GLUT4 present in T-tubules in quadriceps muscles of fasted, transgenic mice compared with controls. Total GLUT4 abundance was slightly decreased likely because of secondary effects on GLUT4 protein stability (9, 12). The absolute increase in GLUT4 in T-tubule membrane fractions was ~3.6-fold, which corresponds well with the ~2.7-fold increase in quadriceps-specific glucose uptake observed *in vivo*. Remarkably, quadriceps-specific glucose uptake in transgenic mice during fasting was similar to that in control mice during hyperinsulinemic-euglycemic clamp studies. There was no significant further effect of the transgene during the clamp studies. In addition, glycogen content was increased ~2.1-fold in quadriceps and ~1.7-fold in gastrocnemius and tibialis anterior. Together with previous results, these data support the idea that insulin-responsive GSVs exist in muscle, that they are regulated by TUG, and that mobilization of these vesicles can account for most of the effect of acute insulin action to increase glucose uptake.

The data imply that endoproteolytic cleavage of TUG is a critical enzymatic mechanism by which insulin regulates GLUT4 in muscle. In 3T3-L1 adipocytes, cleavage requires the TC10α GTPase, which is linked to TUG biochemically through its effector, PIST (15). We isolated the "neuronal" splice variant of PIST from skeletal muscle cDNA; this protein forms a trimeric complex with TUG and GLUT4 and colocalizes with GLUT4 in 3T3-L1 adipocytes (15, 47). PIST and TUG both bind the Golgi matrix protein Golgin-160, which is required for basal GLUT4 intracellular retention (41, 48). Thus, TUG cleavage liberates GSVs trapped at the Golgi matrix. In mTUG$^{UBX\text{-}Cter}$ transgenic mice, PIST was depleted, and TUG cleavage was ongoing during fasting. Together, the data support the idea that PIST inhibits TUG cleavage in the absence of GTP-bound TC10α. Expression of the unstable, PIST-interacting UBX-Cter fragment recruits PIST for degradation, resulting in constitutive TUG cleavage in the transgenic animals. This model accounts for how UBX-Cter acts irreversibly (15) and additionally suggests a mechanism for insulin to stimulate TUG cleavage in wild type mice. Specifically, we propose that binding of GTP-TC10α to PIST displaces or repositions PIST within a protein complex to facilitate TUG endoproteolysis. Testing this model will require additional work.

Insulin signaling through TC10α has not been well studied. The effects of overexpression confounded initial studies using mutated TC10 proteins, and RNAi was required to show definitively that TC10α is required for GLUT4 translocation in 3T3-L1 adipocytes (49–52). The TC10α isoform is highly expressed in muscle and fat and was activated by insulin in most studies (50, 53, 54). Mediators of insulin signaling to TC10α remain uncertain; in particular, disruption of the proposed signaling proteins APS and c-Cbl did not impair, but actually enhanced, insulin action (49, 55–59). Other proteins may mediate upstream signaling (60). Alternatively, APS and c-Cbl may be paradoxical components in a feed-forward circuit that responds to short term changes in insulin concentrations but not to absolute or steady-state insulin concentrations (61). Such circuits typically generate pulse outputs, which may reflect the rate of change of an input signal. This model would fit well with the proposed role of TUG cleavage to release discrete quanta of sequestered GLUT4 into a cell surface recycling pathway rather than to mediate ongoing insulin action during the steady state (3, 15, 23).

Our data highlight the distinction between acute and sustained insulin actions. TUG regulates GLUT4 during fasting and acutely as it is cleaved to release GSVs at the transition from basal to insulin-stimulated states. There was no effect of the UBX-Cter transgene during hyperinsulinemic-euglycemic clamp studies, consistent with data implying that GLUT4 recycles to the cell surface from endosomes during sustained insulin exposure (3, 13, 18). For acute GLUT4 translocation, TC10α-PIST-TUG signaling is likely coordinated with Akt2-AS160-

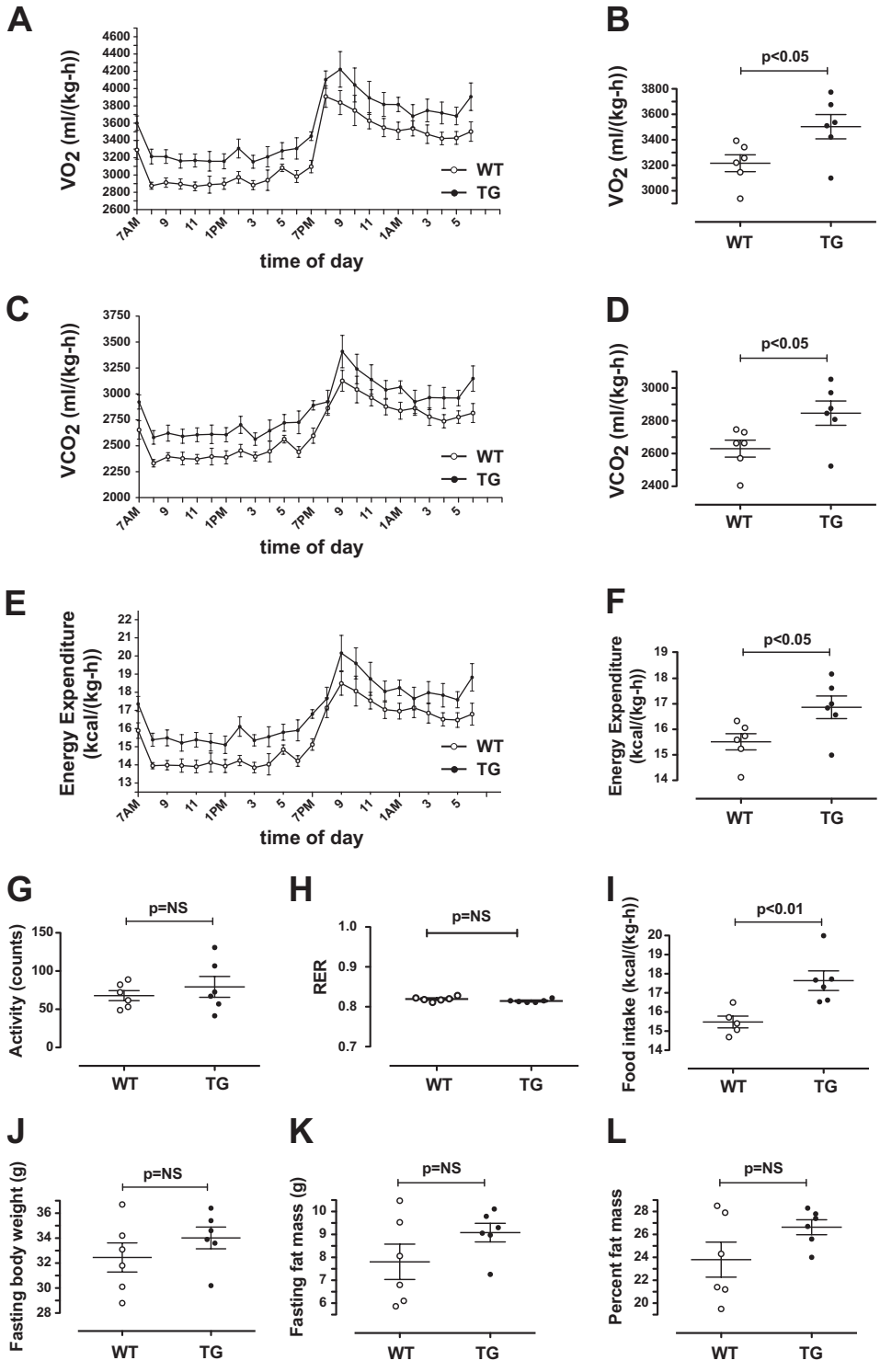

FIGURE 7. **Increased metabolic rate in HFD-fed mTUG$^{UBX\text{-}Cter}$ mice.** Energy metabolism was analyzed in 14-week-old HFD-fed control (WT) and mTUG$^{UBX\text{-}Cter}$ TG mice. *A–D*, VO_2 and VCO_2 were measured and plotted with respect to clock time (*A* and *C*) and as 24-h averages (*B* and *D*). *E* and *F*, energy expenditure was measured by indirect calorimetry and plotted with respect to clock time (*E*) and as a 24-h average (*F*). *G–I*, locomotor activity (beam breaks), averaged RER, and food consumption are plotted. *J–L*, fasting body weight, fat mass, and percent fat mass are plotted. Data are presented as mean ± S.E.; $n = 6$ in each group. *Error bars* represent S.E. *NS*, not significant.

Rab10 signaling to regulate GSVs. During sustained insulin exposure, signaling through Akt2 to Rab14 and other mediators (but not TUG) may direct GLUT4 recycling through endosomes (17, 18, 20, 21, 62). Only when sustained insulin signals are terminated is GLUT4 returned to a TUG-regulated compartment. In fasting mTUG$^{UBX\text{-}Cter}$ mice, the itinerary of GLUT4 is likely similar to ongoing acute insulin action, not to normal sustained insulin action. Endocytosed GLUT4 is targeted to a GSV compartment, but it cannot be retained because of the action of the UBX-Cter transgene. It is thus targeted back

to the cell surface from GSVs, not from endosomes as occurs normally during sustained insulin exposure. Provided that GLUT4 is made available by initial GSV release, the endosome recycling itinerary may be the main one that maintains high levels of GLUT4 at the cell surface during hyperinsulinemic clamp studies.

The effect of insulin to stimulate TUG proteolysis was more dramatic in skeletal muscle than in 3T3-L1 adipocytes, consistent with the observation that cleavage is differentiation-dependent (15). In 3T3-L1 adipocytes, the C-terminal cleavage product was present in both modified (54-kDa) and unmodified (42-kDa) forms. In skeletal muscle, only the unmodified form (~42 kDa) was detected. Possibly, the 54-kDa modified form was not well solubilized under the biochemical conditions required to make muscle lysates. This modification has not been characterized, and further work will be required to understand its physiologic role. However, because the TUG cleavage products may have functions subsequent to their generation and independent of intact TUG, the UBX-Cter protein is not simply a "dominant negative" fragment. By promoting constitutive and unregulated cleavage of intact TUG, the UBX-Cter protein mimics insulin action with respect to both the generation of these products and the mobilization of GLUT4 that resides at a particular site in its overall trafficking itinerary.

Several systemic effects followed from skeletal muscle-specific expression of the UBX-Cter protein that might have been more dramatic but for the limited efficacy of the UBX-Cter transgene in some muscles. We observed decreased plasma glucose and insulin concentrations in $mTUG^{UBX\text{-}Cter}$ mice. These were more marked after a 4–6-h fast than after an overnight fast, consistent with the idea that sensitivity is improved by the shorter fasting duration (44). The lower plasma insulin concentrations may have contributed to the reduced lean body mass we observed, converse to the role of insulin to induce fetal macrosomia in hyperglycemic mothers (63). During fasting, whole-body glucose turnover was increased by 17%, which remained significant when normalized on a per mouse basis, and glycolysis was increased by 15%. The increased turnover was specific to the fasted state. Given that the transgene likely had limited efficacy, the robust effects we observed set a lower bound for the overall role of TUG action in muscle to control whole-body glucose turnover during fasting.

Unexpectedly, the $mTUG^{UBX\text{-}Cter}$ mice had a 12–13% increase in metabolic rate. Similar to transgenic mice overexpressing GLUT1 or GLUT4 in muscle, $mTUG^{UBX\text{-}Cter}$ mice had increased muscle glycogen (64–67). However, in contrast to transgenic mice overexpressing glucose transporters, $mTUG^{UBX\text{-}Cter}$ mice had reduced, not increased, plasma lactate (66, 68–72). Additionally, RER was unchanged in $mTUG^{UBX\text{-}Cter}$ mice, not increased as it is in GLUT4 transgenic mice (66). These metabolic effects may result from action of GSV proteins other than GLUT4 that are coregulated by translocation (3). Alternatively, the TUG C-terminal product may act independently to enhance fuel oxidation. Either way, the data suggest that glucose uptake and energy metabolism may be coupled. Further work will be required to understand this aspect of the phenotype.

Effects of the UBX-Cter transgene were observed in HFD-fed, insulin-resistant mice. In contrast to chow-fed mice, HFD-fed transgenic mice had reduced plasma glucose after an overnight fast compared with wild type controls, and the whole-body glucose turnover was not increased. These phenotypes of chow- and HFD-fed mice may result from similar effects on glucose uptake. If hepatic glucose output is sufficient to maintain euglycemia, then increased turnover is observed as in the chow-fed animals. If hepatic glucose output is limiting, then reduced plasma glucose is observed as in the HFD-fed mice. Our metabolic cage data further support the idea that effects of the UBX-Cter transgene are largely maintained in the setting of HFD-induced insulin resistance. HFD-fed transgenic mice had increased VO_2, VCO_2, and energy expenditure similar to chow-fed mice, and increased food intake was more marked. As in chow-fed animals, there was no effect of the transgene on glucose turnover during hyperinsulinemic clamp studies. Because the main effect of the HFD to induce insulin resistance was observed in hyperinsulinemic clamp studies, the data imply that TUG does not participate in this effect.

We conclude that insulin action at a TUG-regulated trafficking step has a marked effect on overall GLUT4 targeting and glucose uptake in muscle with significance for whole-body glucose turnover. Furthermore, this pathway impacts the overall metabolic rate. Finally, effects on fasting plasma glucose concentrations and energy expenditure are maintained during HFD-induced insulin resistance. These results will lead to an improved understanding of how insulin regulates glucose uptake and how this process may be impaired in type 2 diabetes.

Acknowledgments—We thank James Cresswell, Chenfei Yu, Bradley Rubin, Whitney Harris Brown, David Frederick, and Richard Kibbey (all of Yale University) for technical assistance and helpful discussions and Amira Klip (University of Toronto) and Michael Caplan (Yale University) for reagents. This work used the Molecular, Transgenic, and Cell Biology Cores of the Yale Diabetes Research Center (supported by NIH Grant DK045735), the Yale Mouse Metabolic Phenotyping Center (supported by NIH Grant DK059635), and the Pilot Program and Physiology Core of the Yale O'Brien Kidney Center (supported by NIH Grant DK079310).

REFERENCES

1. Cline, G. W., Petersen, K. F., Krssak, M., Shen, J., Hundal, R. S., Trajanoski, Z., Inzucchi, S., Dresner, A., Rothman, D. L., and Shulman, G. I. (1999) Impaired glucose transport as a cause of decreased insulin-stimulated muscle glycogen synthesis in type 2 diabetes. *N. Engl. J. Med.* **341,** 240–246
2. Minokoshi, Y., Kahn, C. R., and Kahn, B. B. (2003) Tissue-specific ablation of the GLUT4 glucose transporter or the insulin receptor challenges assumptions about insulin action and glucose homeostasis. *J. Biol. Chem.* **278,** 33609–33612
3. Bogan, J. S. (2012) Regulation of glucose transporter translocation in health and diabetes. *Annu. Rev. Biochem.* **81,** 507–532
4. Samuel, V. T., and Shulman, G. I. (2012) Mechanisms for insulin resistance: common threads and missing links. *Cell* **148,** 852–871
5. Garvey, W. T., Maianu, L., Zhu, J. H., Brechtel-Hook, G., Wallace, P., and Baron, A. D. (1998) Evidence for defects in the trafficking and translocation of GLUT4 glucose transporters in skeletal muscle as a cause of human insulin resistance. *J. Clin. Investig.* **101,** 2377–2386
6. Maianu, L., Keller, S. R., and Garvey, W. T. (2001) Adipocytes exhibit

abnormal subcellular distribution and translocation of vesicles containing glucose transporter 4 and insulin-regulated aminopeptidase in type 2 diabetes mellitus: implications regarding defects in vesicle trafficking. *J. Clin. Endocrinol. Metab.* **86,** 5450–5456
7. Vassilopoulos, S., Esk, C., Hoshino, S., Funke, B. H., Chen, C. Y., Plocik, A. M., Wright, W. E., Kucherlapati, R., and Brodsky, F. M. (2009) A role for the CHC22 clathrin heavy-chain isoform in human glucose metabolism. *Science* **324,** 1192–1196
8. Petersen, K. F., Dufour, S., Savage, D. B., Bilz, S., Solomon, G., Yonemitsu, S., Cline, G. W., Befroy, D., Zemany, L., Kahn, B. B., Papademetris, X., Rothman, D. L., and Shulman, G. I. (2007) The role of skeletal muscle insulin resistance in the pathogenesis of the metabolic syndrome. *Proc. Natl. Acad. Sci. U.S.A.* **104,** 12587–12594
9. Rubin, B. R., and Bogan, J. S. (2009) Intracellular retention and insulin-stimulated mobilization of GLUT4 glucose transporters. *Vitam. Horm.* **80,** 155–192
10. Bogan, J. S., and Kandror, K. V. (2010) Biogenesis and regulation of insulin-responsive vesicles containing GLUT4. *Curr. Opin. Cell Biol.* **22,** 506–512
11. Bogan, J. S., Hendon, N., McKee, A. E., Tsao, T. S., and Lodish, H. F. (2003) Functional cloning of TUG as a regulator of GLUT4 glucose transporter trafficking. *Nature* **425,** 727–733
12. Yu, C., Cresswell, J., Löffler, M. G., and Bogan, J. S. (2007) The glucose transporter 4-regulating protein TUG is essential for highly insulin-responsive glucose uptake in 3T3-L1 adipocytes. *J. Biol. Chem.* **282,** 7710–7722
13. Xu, Y., Rubin, B. R., Orme, C. M., Karpikov, A., Yu, C., Bogan, J. S., and Toomre, D. K. (2011) Dual-mode of insulin action controls GLUT4 vesicle exocytosis. *J. Cell Biol.* **193,** 643–653
14. Orme, C. M., and Bogan, J. S. (2012) The ubiquitin regulatory X (UBX) domain-containing protein TUG regulates the p97 ATPase and resides at the endoplasmic reticulum-Golgi intermediate compartment. *J. Biol. Chem.* **287,** 6679–6692
15. Bogan, J. S., Rubin, B. R., Yu, C., Löffler, M. G., Orme, C. M., Belman, J. P., McNally, L. J., Hao, M., and Cresswell, J. A. (2012) Endoproteolytic cleavage of TUG protein regulates GLUT4 glucose transporter translocation. *J. Biol. Chem.* **287,** 23932–23947
16. Cho, H., Mu, J., Kim, J. K., Thorvaldsen, J. L., Chu, Q., Crenshaw, E. B., 3rd, Kaestner, K. H., Bartolomei, M. S., Shulman, G. I., and Birnbaum, M. J. (2001) Insulin resistance and a diabetes mellitus-like syndrome in mice lacking the protein kinase Akt2 (PKBβ). *Science* **292,** 1728–1731
17. Cartee, G. D., and Wojtaszewski, J. F. (2007) Role of Akt substrate of 160 kDa in insulin-stimulated and contraction-stimulated glucose transport. *Appl. Physiol. Nutr. Metab.* **32,** 557–566
18. Chen, Y., Wang, Y., Zhang, J., Deng, Y., Jiang, L., Song, E., Wu, X. S., Hammer, J. A., Xu, T., and Lippincott-Schwartz, J. (2012) Rab10 and myosin-Va mediate insulin-stimulated GLUT4 storage vesicle translocation in adipocytes. *J. Cell Biol.* **198,** 545–560
19. Jewell, J. L., Oh, E., Ramalingam, L., Kalwat, M. A., Tagliabracci, V. S., Tackett, L., Elmendorf, J. S., and Thurmond, D. C. (2011) Munc18c phosphorylation by the insulin receptor links cell signaling directly to SNARE exocytosis. *J. Cell Biol.* **193,** 185–199
20. Lansey, M. N., Walker, N. N., Hargett, S. R., Stevens, J. R., and Keller, S. R. (2012) Deletion of Rab GAP AS160 modifies glucose uptake and GLUT4 translocation in primary skeletal muscles and adipocytes and impairs glucose homeostasis. *Am. J. Physiol. Endocrinol. Metab.* **303,** E1273–E1286
21. Wang, H. Y., Ducommun, S., Quan, C., Xie, B., Li, M., Wasserman, D. H., Sakamoto, K., Mackintosh, C., and Chen, S. (2013) AS160 deficiency causes whole-body insulin resistance via composite effects in multiple tissues. *Biochem. J.* **449,** 479–489
22. Hatakeyama, H., and Kanzaki, M. (2013) Regulatory mode shift of Tbc1d1 is required for acquisition of insulin-responsive GLUT4-trafficking activity. *Mol. Biol. Cell* **24,** 809–817
23. Govers, R., Coster, A. C., and James, D. E. (2004) Insulin increases cell surface GLUT4 levels by dose dependently discharging GLUT4 into a cell surface recycling pathway. *Mol. Cell. Biol.* **24,** 6456–6466
24. Thurmond, D. C., and Pessin, J. E. (2000) Discrimination of GLUT4 vesicle trafficking from fusion using a temperature-sensitive Munc18c mutant. *EMBO J.* **19,** 3565–3575
25. Hatakeyama, H., and Kanzaki, M. (2011) Molecular basis of insulin-responsive GLUT4 trafficking systems revealed by single molecule imaging. *Traffic* **12,** 1805–1820
26. Schertzer, J. D., Antonescu, C. N., Bilan, P. J., Jain, S., Huang, X., Liu, Z., Bonen, A., and Klip, A. (2009) A transgenic mouse model to study glucose transporter 4myc regulation in skeletal muscle. *Endocrinology* **150,** 1935–1940
27. Castorena, C. M., Mackrell, J. G., Bogan, J. S., Kanzaki, M., and Cartee, G. D. (2011) Clustering of GLUT4, TUG, and RUVBL2 protein levels correlate with myosin heavy chain isoform pattern in skeletal muscles, but AS160 and TBC1D1 levels do not. *J. Appl. Physiol.* **111,** 1106–1117
28. Jaynes, J. B., Johnson, J. E., Buskin, J. N., Gartside, C. L., and Hauschka, S. D. (1988) The muscle creatine kinase gene is regulated by multiple upstream elements, including a muscle-specific enhancer. *Mol. Cell. Biol.* **8,** 62–70
29. Donoviel, D. B., Shield, M. A., Buskin, J. N., Haugen, H. S., Clegg, C. H., and Hauschka, S. D. (1996) Analysis of muscle creatine kinase gene regulatory elements in skeletal and cardiac muscles of transgenic mice. *Mol. Cell. Biol.* **16,** 1649–1658
30. Nguyen, Q. G., Buskin, J. N., Himeda, C. L., Shield, M. A., and Hauschka, S. D. (2003) Differences in the function of three conserved E-boxes of the muscle creatine kinase gene in cultured myocytes and in transgenic mouse skeletal and cardiac muscle. *J. Biol. Chem.* **278,** 46494–46505
31. Hong, E. G., Ko, H. J., Cho, Y. R., Kim, H. J., Ma, Z., Yu, T. Y., Friedline, R. H., Kurt-Jones, E., Finberg, R., Fischer, M. A., Granger, E. L., Norbury, C. C., Hauschka, S. D., Philbrick, W. M., Lee, C. G., Elias, J. A., and Kim, J. K. (2009) Interleukin-10 prevents diet-induced insulin resistance by attenuating macrophage and cytokine response in skeletal muscle. *Diabetes* **58,** 2525–2535
32. Jurczak, M. J., Lee, A. H., Jornayvaz, F. R., Lee, H. Y., Birkenfeld, A. L., Guigni, B. A., Kahn, M., Samuel, V. T., Glimcher, L. H., and Shulman, G. I. (2012) Dissociation of inositol-requiring enzyme (IRE1α)-mediated c-Jun N-terminal kinase activation from hepatic insulin resistance in conditional X-box-binding protein-1 (XBP1) knock-out mice. *J. Biol. Chem.* **287,** 2558–2567
33. Ayala, J. E., Samuel, V. T., Morton, G. J., Obici, S., Croniger, C. M., Shulman, G. I., Wasserman, D. H., and McGuinness, O. P. (2010) Standard operating procedures for describing and performing metabolic tests of glucose homeostasis in mice. *Dis. Model. Mech.* **3,** 525–534
34. Youn, J. H., and Buchanan, T. A. (1993) Fasting does not impair insulin-stimulated glucose uptake but alters intracellular glucose metabolism in conscious rats. *Diabetes* **42,** 757–763
35. Choi, C. S., Savage, D. B., Abu-Elheiga, L., Liu, Z. X., Kim, S., Kulkarni, A., Distefano, A., Hwang, Y. J., Reznick, R. M., Codella, R., Zhang, D., Cline, G. W., Wakil, S. J., and Shulman, G. I. (2007) Continuous fat oxidation in acetyl-CoA carboxylase 2 knockout mice increases total energy expenditure, reduces fat mass, and improves insulin sensitivity. *Proc. Natl. Acad. Sci. U.S.A.* **104,** 16480–16485
36. Zhang, B., Arun, G., Mao, Y. S., Lazar, Z., Hung, G., Bhattacharjee, G., Xiao, X., Booth, C. J., Wu, J., Zhang, C., and Spector, D. L. (2012) The lncRNA Malat1 is dispensable for mouse development but its transcription plays a cis-regulatory role in the adult. *Cell Rep.* **2,** 111–123
37. Bogan, J. S., McKee, A. E., and Lodish, H. F. (2001) Insulin-responsive compartments containing GLUT4 in 3T3-L1 and CHO cells: regulation by amino acid concentrations. *Mol. Cell. Biol.* **21,** 4785–4806
38. Zorzano, A., and Camps, M. (2006) Isolation of T-tubules from skeletal muscle. *Curr. Protoc. Cell Biol.* **Chapter 3,** Unit 3.24
39. Pietrini, G., Matteoli, M., Banker, G., and Caplan, M. J. (1992) Isoforms of the Na,K-ATPase are present in both axons and dendrites of hippocampal neurons in culture. *Proc. Natl. Acad. Sci. U.S.A.* **89,** 8414–8418
40. Rechsteiner, M., and Rogers, S. W. (1996) PEST sequences and regulation by proteolysis. *Trends Biochem. Sci.* **21,** 267–271
41. Hicks, S. W., and Machamer, C. E. (2005) Isoform-specific interaction of golgin-160 with the Golgi-associated protein PIST. *J. Biol. Chem.* **280,** 28944–28951
42. Sbodio, J. I., Hicks, S. W., Simon, D., and Machamer, C. E. (2006) GCP60 preferentially interacts with a caspase-generated golgin-160 fragment. *J. Biol. Chem.* **281,** 27924–27931

43. Sbodio, J. I., and Machamer, C. E. (2007) Identification of a redox-sensitive cysteine in GCP60 that regulates its interaction with golgin-160. *J. Biol. Chem.* **282,** 29874–29881
44. Andrikopoulos, S., Blair, A. R., Deluca, N., Fam, B. C., and Proietto, J. (2008) Evaluating the glucose tolerance test in mice. *Am. J. Physiol. Endocrinol. Metab.* **295,** E1323–E1332
45. Park, S. Y., Kim, H. J., Wang, S., Higashimori, T., Dong, J., Kim, Y. J., Cline, G., Li, H., Prentki, M., Shulman, G. I., Mitchell, G. A., and Kim, J. K. (2005) Hormone-sensitive lipase knockout mice have increased hepatic insulin sensitivity and are protected from short-term diet-induced insulin resistance in skeletal muscle and heart. *Am. J. Physiol. Endocrinol. Metab.* **289,** E30–E39
46. Zhang, D., Christianson, J., Liu, Z. X., Tian, L., Choi, C. S., Neschen, S., Dong, J., Wood, P. A., and Shulman, G. I. (2010) Resistance to high-fat diet-induced obesity and insulin resistance in mice with very long-chain acyl-CoA dehydrogenase deficiency. *Cell Metab.* **11,** 402–411
47. Yue, Z., Horton, A., Bravin, M., DeJager, P. L., Selimi, F., and Heintz, N. (2002) A novel protein complex linking the δ2 glutamate receptor and autophagy: implications for neurodegeneration in lurcher mice. *Neuron* **35,** 921–933
48. Williams, D., Hicks, S. W., Machamer, C. E., and Pessin, J. E. (2006) Golgin-160 is required for the Golgi membrane sorting of the insulin-responsive glucose transporter GLUT4 in adipocytes. *Mol. Biol. Cell* **17,** 5346–5355
49. Chiang, S. H., Baumann, C. A., Kanzaki, M., Thurmond, D. C., Watson, R. T., Neudauer, C. L., Macara, I. G., Pessin, J. E., and Saltiel, A. R. (2001) Insulin-stimulated GLUT4 translocation requires the CAP-dependent activation of TC10. *Nature* **410,** 944–948
50. JeBailey, L., Rudich, A., Huang, X., Di Ciano-Oliveira, C., Kapus, A., and Klip, A. (2004) Skeletal muscle cells and adipocytes differ in their reliance on TC10 and Rac for insulin-induced actin remodeling. *Mol. Endocrinol.* **18,** 359–372
51. Chiang, S. H., Chang, L., and Saltiel, A. R. (2006) TC10 and insulin-stimulated glucose transport. *Methods Enzymol.* **406,** 701–714
52. Chang, L., Chiang, S. H., and Saltiel, A. R. (2007) TC10α is required for insulin-stimulated glucose uptake in adipocytes. *Endocrinology* **148,** 27–33
53. Neudauer, C. L., Joberty, G., Tatsis, N., and Macara, I. G. (1998) Distinct cellular effects and interactions of the Rho-family GTPase TC10. *Curr. Biol.* **8,** 1151–1160
54. Gupte, A., and Mora, S. (2006) Activation of the Cbl insulin signaling pathway in cardiac muscle; dysregulation in obesity and diabetes. *Biochem. Biophys. Res. Commun.* **342,** 751–757
55. Liu, J., Kimura, A., Baumann, C. A., and Saltiel, A. R. (2002) APS facilitates c-Cbl tyrosine phosphorylation and GLUT4 translocation in response to insulin in 3T3-L1 adipocytes. *Mol. Cell. Biol.* **22,** 3599–3609
56. Ahn, M. Y., Katsanakis, K. D., Bheda, F., and Pillay, T. S. (2004) Primary and essential role of the adaptor protein APS for recruitment of both c-Cbl and its associated protein CAP in insulin signaling. *J. Biol. Chem.* **279,** 21526–21532
57. Mitra, P., Zheng, X., and Czech, M. P. (2004) RNAi-based analysis of CAP, Cbl, and CrkII function in the regulation of GLUT4 by insulin. *J. Biol. Chem.* **279,** 37431–37435
58. Minami, A., Iseki, M., Kishi, K., Wang, M., Ogura, M., Furukawa, N., Hayashi, S., Yamada, M., Obata, T., Takeshita, Y., Nakaya, Y., Bando, Y., Izumi, K., Moodie, S. A., Kajiura, F., Matsumoto, M., Takatsu, K., Takaki, S., and Ebina, Y. (2003) Increased insulin sensitivity and hypoinsulinemia in APS knockout mice. *Diabetes* **52,** 2657–2665
59. Molero, J. C., Jensen, T. E., Withers, P. C., Couzens, M., Herzog, H., Thien, C. B., Langdon, W. Y., Walder, K., Murphy, M. A., Bowtell, D. D., James, D. E., and Cooney, G. J. (2004) c-Cbl-deficient mice have reduced adiposity, higher energy expenditure, and improved peripheral insulin action. *J. Clin. Investig.* **114,** 1326–1333
60. Liu, J., DeYoung, S. M., Hwang, J. B., O'Leary, E. E., and Saltiel, A. R. (2003) The roles of Cbl-b and c-Cbl in insulin-stimulated glucose transport. *J. Biol. Chem.* **278,** 36754–36762
61. Hart, Y., and Alon, U. (2013) The utility of paradoxical components in biological circuits. *Mol. Cell* **49,** 213–221
62. Szekeres, F., Chadt, A., Tom, R. Z., Deshmukh, A. S., Chibalin, A. V., Björnholm, M., Al-Hasani, H., and Zierath, J. R. (2012) The Rab-GTPase-activating protein TBC1D1 regulates skeletal muscle glucose metabolism. *Am. J. Physiol. Endocrinol Metab.* **303,** E524–E533
63. Langer, O. (2000) Fetal macrosomia: etiologic factors. *Clin. Obstet. Gynecol.* **43,** 283–297
64. Gulve, E. A., Ren, J. M., Marshall, B. A., Gao, J., Hansen, P. A., Holloszy, J. O., and Mueckler, M. (1994) Glucose transport activity in skeletal muscles from transgenic mice overexpressing GLUT1. Increased basal transport is associated with a defective response to diverse stimuli that activate GLUT4. *J. Biol. Chem.* **269,** 18366–18370
65. Liu, M. L., Gibbs, E. M., McCoid, S. C., Milici, A. J., Stukenbrok, H. A., McPherson, R. K., Treadway, J. L., and Pessin, J. E. (1993) Transgenic mice expressing the human GLUT4/muscle-fat facilitative glucose transporter protein exhibit efficient glycemic control. *Proc. Natl. Acad. Sci. U.S.A.* **90,** 11346–11350
66. Bao, S., and Garvey, W. T. (1997) Exercise in transgenic mice overexpressing GLUT4 glucose transporters: effects on substrate metabolism and glycogen regulation. *Metabolism* **46,** 1349–1357
67. Brozinick, J. T., Jr., McCoid, S. C., Reynolds, T. H., Wilson, C. M., Stevenson, R. W., Cushman, S. W., and Gibbs, E. M. (1997) Regulation of cell surface GLUT4 in skeletal muscle of transgenic mice. *Biochem. J.* **321,** 75–81
68. Treadway, J. L., Hargrove, D. M., Nardone, N. A., McPherson, R. K., Russo, J. F., Milici, A. J., Stukenbrok, H. A., Gibbs, E. M., Stevenson, R. W., and Pessin, J. E. (1994) Enhanced peripheral glucose utilization in transgenic mice expressing the human GLUT4 gene. *J. Biol. Chem.* **269,** 29956–29961
69. Hansen, P. A., Gulve, E. A., Marshall, B. A., Gao, J., Pessin, J. E., Holloszy, J. O., and Mueckler, M. (1995) Skeletal muscle glucose transport and metabolism are enhanced in transgenic mice overexpressing the Glut4 glucose transporter. *J. Biol. Chem.* **270,** 1679–1684
70. Deems, R. O., Evans, J. L., Deacon, R. W., Honer, C. M., Chu, D. T., Bürki, K., Fillers, W. S., Cohen, D. K., and Young, D. A. (1994) Expression of human GLUT4 in mice results in increased insulin action. *Diabetologia* **37,** 1097–1104
71. Tsao, T. S., Burcelin, R., Katz, E. B., Huang, L., and Charron, M. J. (1996) Enhanced insulin action due to targeted GLUT4 overexpression exclusively in muscle. *Diabetes* **45,** 28–36
72. Ren, J. M., Marshall, B. A., Mueckler, M. M., McCaleb, M., Amatruda, J. M., and Shulman, G. I. (1995) Overexpression of Glut4 protein in muscle increases basal and insulin-stimulated whole-body glucose disposal in conscious mice. *J. Clin. Investig.* **95,** 429–432